Photochemistry of $M(PP_3)H_2$ (M = Ru, Os; PP_3 = $P(CH_2CH_2PPh_2)_3$): Preparative, NMR, and Time-Resolved Studies

Robert Osman,[†] David I. Pattison,[†] Robin N. Perutz,*[,†] Claudio Bianchini,*[,‡] Juan A. Casares,[‡,§] and Maurizio Peruzzini[‡]

Contribution from the Department of Chemistry, University of York, Heslington, York, YO1 5DD, U.K., and the Istituto per lo Studio della Stereochimica ed Energetica dei Composti di Coordinazione, ISSECC-CNR, Via J. Nardi 39, 50132 Firenze, Italy

Received October 31, 1996[⊗]

Abstract: Photochemical reaction of $Ru(PP_3)H_2$ ($PP_3 = P(CH_2CH_2PPh_2)_3$) in THF under a rigorously inert atmosphere yields the cyclometalated complex $Ru[(Ph_2PCH_2CH_2)_2P(CH_2CH_2PPhC_6H_4)]H$. The latter is converted back to $Ru(PP_3)H_2$ under H_2 and reacts even with traces of N_2 to yield $Ru(PP_3)(N_2)$. The dinitrogen complex may be synthesized directly by a number of methods. NMR spectroscopy shows that photolysis of $Ru(PP_3)H_2$ under C_2H_4 and CO yields $Ru(PP_3)(C_2H_4)$ and $Ru(PP_3)(CO)$, respectively. Photolysis of $Ru(PP_3)H_2$ with $HSiEt_3$ in THF yields $Ru(PP_3)(SiEt_3)H$, while photolysis in mixtures of THF and benzene at low temperature yields $Ru(PP_3)(Ph)H$. The latter is also generated by reduction of $Ru(PP_3)Cl_2$ in the presence of benzene. $Os(PP_3)(Ph)H$ is formed either by photolysis of $Os(PP_3)H_2$ or by reduction of $Os(PP_3)Cl_2$ in the presence of benzene. Irradiation of $Os(PP_3)H_2$ in THF or THF/hexane mixtures initially yields the THF C−H activation product, $Os(PP_3)(2\text{-}C_4H_7O)H$. This complex is also generated by reduction of $Os(PP_3)Cl_2$ with sodium naphthalenide under N_2 in the presence of THF. $Os(PP_3)(2\text{-}C_4H_7O)H$ is converted to the cyclometalated complex, $Os[(Ph_2PCH_2CH_2)_2P(CH_2CH_2PPhC_6H_4)]H$, on irradiation in THF and to $Os(PP_3)(Ph)H$ on irradiation in benzene. Reaction of $Os(PP_3)H_2$ with CH_3OTf (Tf = triflate) yields $Os(PP_3)(OTf)H$, which is converted to the labile $Os(PP_3)(CH_3)H$ on reaction with methyllithium. Laser flash photolysis of $Ru(PP_3)H_2$ in cyclohexane (laser wavelength 308 nm) yields transient $Ru(PP_3)$ with an absorption maximum at 395 nm. The transient reacts with H_2, C_6H_6, $HSiEt_3$, CO, N_2, C_2H_4, and THF with little discrimination; the second-order rate constants for these reactions lie in the range $5 \times 10^5-2 \times 10^6$ dm^3 mol^{-1} s^{-1} at 295 K. Kinetic isotope effects have been determined for the reaction with benzene and THF, as 1.5 (0.2) and 1.1 (0.2), respectively. Activation parameters for reaction of $Ru(PP_3)$ are as follows: with $HSiEt_3$ $\Delta H^{\ddagger} = 35$ (2) kJ mol^{-1}, $\Delta S^{\ddagger} = -18$ (6) J K^{-1} mol^{-1}; with C_6H_6 $\Delta H^{\ddagger} = 39$ (4) kJ mol^{-1}, $\Delta S^{\ddagger} \approx 0$ J K^{-1} mol^{-1}. The reaction with THF yields a short-lived adduct, probably bound through oxygen, which is rapidly converted to the cyclometalated product. Laser flash photolysis of $Os(PP_3)H_2$ generates transient $Os(PP_3)$ ($\lambda_{max} = 390$ nm). The transient kinetics of $Os(PP_3)$ are substantially different from its ruthenium analogue. It reacts with alkanes and shows different behavior toward THF but is unaffected by addition of H_2. Rate constants in the range $6 \times 10^4-6 \times 10^5$ dm^3 mol^{-1} s^{-1} (295 K) are presented for reaction with C_6H_6, THF, $HSiEt_3$, CO, C_2H_4, N_2, and several alkanes. Kinetic isotope effects have been determined for the reactions with methylcyclohexane and benzene as 5.6 (1.5) and 0.6 (0.1), respectively. The rate constants for reaction with alkanes rise in the order, methylcyclohexane < pentane < heptane < methane. The rate constants for reaction with methane and benzene are insignificantly different. Following reaction of $Os(PP_3)$ with THF to form $Os(PP_3)(THF)$, C−H insertion occurs with a first-order rate constant of 4.2 (8) $\times 10^3$ s^{-1} with $k_H/k_D = 2.6$ (0.4). The activation parameters for reaction of $Os(PP_3)$ with substrates are as follows: with pentane $\Delta H^{\ddagger} = 27$ (1) kJ mol^{-1}, $\Delta S^{\ddagger} = -59$ (4) J K^{-1} mol^{-1}; with $HSiEt_3$ $\Delta H^{\ddagger} = 31$ (5) kJ mol^{-1}, $\Delta S^{\ddagger} = -27$ (12) J K^{-1} mol^{-1}; with C_6H_6 $\Delta H^{\ddagger} = 38$ (3) kJ mol^{-1}, $\Delta S^{\ddagger} = -7$ (9) J K^{-1} mol^{-1}.

Introduction

Photochemical elimination of dihydrogen from metal dihydride complexes dates back to the discovery of the photoreaction of $W(\eta^5\text{-}C_5H_5)_2H_2$ with benzene by Giannotti and Green.[1] The photochemical methods[2] were soon found to complement the more traditional reductive syntheses, for instance of dimers of $Mo(\eta^5\text{-}C_5H_5)_2$.[3] In recent years, photochemical elimination of dihydrogen has become one of the key routes into carbon−hydrogen bond activation especially by half-sandwich rhodium, iridium, and osmium complexes.[4−6] One advantage of the photochemical method lies in the ability to obtain kinetic data by laser flash photolysis. We recently exploited this in our

[†] University of York.
[‡] ISSECC, Florence.
[§] Present address: Departamento de Quimica Inorganica, Universidad de Valladolid, Spain.
[⊗] Abstract published in *Advance ACS Abstracts,* August 15, 1997.

(1) Giannotti, C.; Green, M. L. H. *J. Chem. Soc. Chem. Commun.* **1972**, 1114.

(2) (a) Berry, M.; Elmitt, K.; Green, M. L. H.; Simpson, S. J. *J. Chem. Soc., Dalton Trans.* **1979**, 1950. (b) Berry, M.; Cooper, N. J.; Green, M. L. H. *J. Chem. Soc., Dalton Trans.* **1980**, 29. (c) Geoffroy, G. L.; Bradley, M. G. *Inorg. Chem.* **1978**, *17*, 2410. (d) Belmore, K. A.; Vanderpool, R. A.; Tsai, J. C.; Khan, M. A.; Nicholas, K. M. *J. Am. Chem. Soc.* **1988**, *110*, 2004. (e) Grebenik, P.; Grinter, R.; Perutz, R. N. *Chem. Soc. Rev.* **1988**, *17*, 453.

(3) (a) Thomas, J. L.; Brintzinger, H. H. *J. Am. Chem. Soc.* **1972**, *94*, 1386. (b) Thomas, J. L. *J. Am. Chem. Soc.* **1973**, *95*, 1838. (c) Bashkin, J.; Green, M. L. H.; Poveda, M. L.; Prout, K. *J. Chem. Soc., Dalton Trans.* **1982**, 2485. (d) Chatt, J.; Davidson, J. M. *J. Chem. Soc.* **1965**, 843.

(4) (a) Jones, W. D.; Feher, F. J. *J. Am. Chem. Soc.* **1984**, *106*, 1650. (b) Jones, W. D.; Feher, F. J. *Acc. Chem. Res.* **1989**, *22*, 91. (c) Periana, R. A.; Bergman, R. G. *J. Am. Chem. Soc.* **1986**, *108*, 7332. (d) Chin, R. M.; Dong, L.; Duckett, S. B.; Partridge, M. G.; Jones, W. D.; Perutz, R. N. *ibid* **1993**, *115*, 7685.

S0002-7863(96)03797-3 CCC: $14.00

Scheme 1. Structures of $M(PP_3)$ and $M(dmpe)_2$

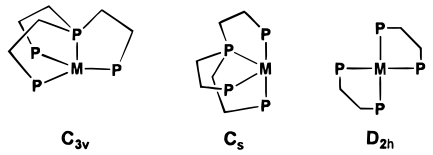

studies of complexes of the type $Ru(R_2PCH_2CH_2PR_2)_2H_2$ (R = Me, Et, Ph, C_2F_5).[7,8] We showed that each of these complexes undergoes photodissociation of dihydrogen to yield 16-electron $Ru(R_2PCH_2CH_2PR_2)_2$ fragments with characteristic multiband UV/vis spectra. The fragments, $Ru(dmpe)_2$, $Ru(depe)_2$, and $Ru(dppe)_2$ (those with R = Me, Et, and Ph, respectively, collectively abbreviated to $Ru(drpe)_2$), are close to square planar and each exhibits a very low energy absorption band at ca. 740 nm. The lowest energy absorption of $Ru(dfepe)_2$ (the analogue with $R = C_2F_5$) is shifted to 620 nm and may be perturbed by F-coordination. The reactivity of $Ru(dmpe)_2$ varies with substrate according to the pattern $k(H_2) > k(CO) > k(C_2H_4) \approx k(HSiEt_3)$. The rate constant for reaction with H_2 is 6.2×10^9 dm^3 mol^{-1} s^{-1}, remarkably close to the diffusion limit. The reactivity of $Ru(depe)_2$ follows the same pattern as for $Ru(dmpe)_2$, but the rate constants are a factor of 15 lower for H_2 and 200 times lower for $HSiEt_3$. The phenyl analogue, $Ru(dppe)_2$, is less reactive still; $k(H_2)$ is 250 times smaller than for $Ru(dmpe)_2$ and $k(C_2H_4)$ is 3700 times smaller, while there is no detectable reaction toward $HSiEt_3$. NMR studies of the photoproducts complement the flash photolysis measurements by allowing conclusive identification of the final products. The flash photolysis and NMR measurements agree for $Ru(depe)_2$, $Ru(dppe)_2$, and $Ru(dfepe)_2$ in showing no reaction with benzene. However, there is a discrepancy between the methods for $Ru(dmpe)_2$: no reaction with benzene is found by laser flash photolysis, but NMR studies show formation of $Ru(dmpe)_2(Ph)H$.

The synthesis of $M(PP_3)H_2$ ($PP_3 = P(CH_2CH_2PPh_2)_3$, M = Ru, Os) complexes[9,10] offered the opportunity to study how the reactivity and spectra of the constrained $M(PP_3)$ unit compare with those of $Ru(drpe)_2$. The tetradentate ligand allows the $M(PP_3)$ transient to adopt pyramidal (C_{3v}) or butterfly (C_s) geometries but prevents adoption of the square planar (D_{2h}) structure characteristic of $Ru(drpe)_2$ (Scheme 1). The numbering of the compounds is shown in Chart 1.

Chart 1. Key to the Compound Numbering System

compound	number	compound	number
$M(PP_3)H_2$	**1Ru/1Os**	$Os(PP_3)(2\text{-}C_4H_7O)H$	**8Os**
$M(PP_3)Cl_2$	**2Ru/2Os**	$M(PP_3)(Cl)H$	**9Ru/9Os**
$[Ru(PP_3)(H)(N_2)]BPh_4$	**3Ru**	$M(PP_3)(C_2H_4)$	**10Ru/10Os**
$M[(Ph_2PCH_2CH_2)_2P\text{-}(CH_2CH_2PPhC_6H_4)]H$	**4Ru/4Os**	$Ru(PP_3)(SiEt_3)H$	**11Ru**
$M(PP_3)(Ph)H$	**5Ru/5Os**	$Os(PP_3)(OTf)H$	**12Os**
$M(PP_3)(N_2)$	**6Ru/6Os**	$Os(PP_3)(Me)H$	**13Os**
$M(PP_3)(CO)$	**7Ru/7Os**		

The Florence group has already obtained considerable information concerning the conversion of $M(PP_3)H_2$ to dihydrogen hydride cations, $[M(PP_3)(\eta^2\text{-}H_2)H]^+$, and other cationic complexes, $[M(PP_3)(L)H]^+$ (M = Ru, Os; L = CO, N_2).[9,10] The cation, $[Rh(PP_3)H_2]^+$, which is isoelectronic with $Ru(PP_3)H_2$, has also been isolated and can be converted to the triflate-stabilized Rh^I species, $[Rh(PP_3)(OSO_2CF_3)]^+$.[11a] The latter coordinates CO, phosphines, and halides and also undergoes oxidative addition with dihydrogen. However, $[Rh(PP_3)(OSO_2CF_3)]^+$ neither undergoes cyclometalation nor reaction with benzene. Intermolecular C−H activation of benzene or THF can be achieved with $[Ir(PP_3)]^+$ [11b] or $[Rh(NP_3)]^+$ ($NP_3 = N(CH_2CH_2PPh_2)_3$).[11a] The fluxional behavior of complexes of the type $[M(PP_3)H_2]^{n+}$ has been reported.[9,10,12]

In this paper we explore the photochemistry of $Ru(PP_3)H_2$ (**1Ru**) and $Os(PP_3)H_2$ (**1Os**) by preparative and by in situ NMR methods. We show that some of the products can also be obtained by thermal routes involving reduction of $M(PP_3)Cl_2$ in the presence of suitable substrates or reaction of $Os(PP_3)H_2$ with methyl triflate. The rates of reaction of $M(PP_3)$ are quantified by laser flash photolysis. Striking features include (a) the scavenging of N_2 by the product of cyclometalation of $Ru(PP_3)$; (b) the completely different kinetic selectivity of $Ru(PP_3)$ and $Os(PP_3)$ compared to $Ru(dppe)_2$; (c) the enhanced reactivity of $Ru(PP_3)$ toward benzene and $HSiEt_3$ compared to $Ru(dppe)_2$; and (d) the insertion of $Os(PP_3)$ into aliphatic C−H bonds of THF and alkanes, most notably of methane itself. Some of the results with $Os(PP_3)$ have been published as a communication.[13]

Experimental Section

Laser Flash Photolysis. The laser flash photolysis apparatus at York has been fully described previously.[7] In summary, a XeCl excimer laser (308 nm) is used as the excitation source, while detection is achieved with a pulsed Xe arc lamp, monochromator, and photomultiplier. The photomultiplier is linked to a digital oscilloscope (Tektronix TDS520), and the system is controlled by a Dell PC with in-house software. Typically, transient data are collected as averages of between two and ten shots. Pseudo-first-order decays were analyzed by fitting a straight line plot of ln ΔA against time using in-house software, while Microcal Origin was used to fit decays to complex analytical expressions, and Simula was used to model decays where no analytical function could be derived.

Samples were prepared in a 10 mm quartz cuvette, fitted with a Young's PTFE stopcock and a degassing bulb. Solid was loaded into these cells in an argon atmosphere glovebox. Solvents (Aldrich HPLC grade) were dried over CaH_2 at reflux and stored under argon. These were transferred to the flash cells via cannula through a silicone septum on a Schlenk line fitted with a mercury diffusion pump. The concentration of the samples was adjusted to obtain an absorbance of 0.6−1.0 at 308 nm and then degassed by three freeze−pump−thaw cycles (to 10^{-4} mbar), before backfilling with the required atmosphere. Gas mixtures were made up manometrically in 1 L bulbs to a pressure of typically 700 Torr. Liquid quenchers were usually prepared as 1 mol dm^{-3} stock solutions, before addition to the samples with a microliter syringe. UV/visible spectra were recorded before and after laser flash photolysis on a Perkin-Elmer Lambda 7G spectrometer.

General Procedures. Solvents (THF, benzene, hexane) were of AR grade and dried by distillation over sodium/benzophenone under an Ar or N_2 atmosphere, while THF was also dried and purified by distillation under nitrogen over $LiAlH_4$. The solvents were stored over

(5) (a) Janowicz, A. H.; Bergman, R. G. *J. Am. Chem. Soc.* **1983**, *105*, 3929. (b) Buchanan, J. M.; Stryker, J. M.; Bergman, R. G. *J. Am. Chem. Soc.* **1986**, *108*, 1537. (c) Sponsler, M. B.; Weiller, B. H.; Stoutland, P. O.; Bergman, R. G. *J. Am. Chem. Soc.* **1989**, *111*, 6841. (d) Bloyce, P. E.; Rest, A. J.; Whitwell, I. *J. Chem. Soc., Dalton Trans.* **1990**, 813. (e) Partridge, M. G.; McCamley, A.; Perutz, R. N. *J. Chem. Soc., Dalton Trans.* **1994**, 3519.

(6) (a) Kiel, W. A.; Ball, R. G.; Graham, W. A. G. *J. Organomet. Chem.* **1990**, *383*, 481. (b) Brough, S. A.; Hall, C.; McCamley, A.; Perutz, R. N.; Stahl, S.; Wecker, U.; Werner, H. *J. Organomet. Chem.* **1995**, *504*, 33.

(7) Hall, C.; Jones, W. D.; Mawby, R. J.; Osman, R.; Perutz, R. N.; Whittlesey, M. K. *J. Am. Chem. Soc.* **1992**, *114*, 7425.

(8) Cronin, L.; Nicasio, M. C.; Perutz, R. N.; Peters, R. G.; Roddick, D. M.; Whittlesey, M. K. *J. Am. Chem. Soc.* **1995**, *117*, 10047.

(9) Bianchini, C.; Perez, P. J.; Peruzzini, M.; Zanobini, F.; Vacca, A. *Inorg. Chem.* **1991**, *30*, 279.

(10) Bianchini, C.; Linn, K.; Masi, D.; Peruzzini, M.; Polo, A.; Vacca, A.; Zanobini, F. *Inorg. Chem.* **1993**, *32*, 2366.

(11) (a) Bianchini, C.; Masi, D.; Meli, A.; Peruzzini, M.; Zanobini, F. *J. Am. Chem. Soc.* **1988**, *110*, 6411. (b) Bianchini, C.; Peruzzini, M.; Zanobini, F. *J. Organomet. Chem.* **1987**, *326*, C79.

(12) Heinekey, D. M.; van Roon, M. *J. Am. Chem. Soc.* **1996**, *118*, 12134.

(13) Osman, R.; Pattison, D. I.; Perutz, R. N.; Bianchini, C.; Peruzzini, M. *J. Chem. Soc., Chem. Commun.* **1994**, 513.

molecular sieves or under argon in ampoules fitted with a PTFE stopcock. *tert*-Butyllithium (1.7 mol dm^{-3} solution in pentane) and phenyllithium (1.8 mol dm^{-3} solution in cyclohexane−diethyl ether) were purchased from Aldrich and used as received. The complexes Ru(PP$_3$)H$_2$ (**1Ru**),[9] Os(PP$_3$)H$_2$ (**1Os**),[10] Ru(PP$_3$)Cl$_2$ (**2Ru**),[9] Os(PP$_3$)-Cl$_2$ (**2Os**),[10] and [Ru(PP$_3$)(H)(N$_2$)]BPh$_4$ (**3Ru**)[9] were prepared as described in the literature. The gases (N$_2$, Ar, C$_2$H$_4$, CH$_4$, H$_2$, CO) were of BOC Research grade (99.999%) or high purity grade (He), while ^{15}N$_2$ (99%) was obtained from MSD Isotopes. Deuterated solvents for NMR measurements (Aldrich, Merck and Goss Scientific Instruments Ltd.) were dried over molecular sieves, or by stirring over potassium/benzophenone before being distilled and stored under vacuum. All reactions and manipulations were routinely performed under a dry nitrogen or argon atmosphere using standard Schlenk, high vacuum line and glovebox techniques. The solid complexes were collected on sintered glass-frits and washed with hexane before being dried in a stream of nitrogen.

Preparative photochemical reactions were performed by using a Helios Italquartz UV 13F apparatus. The photolysis source was a 135 W (principal emission wavelength at 366 nm) high-pressure mercury vapor immersion lamp equipped with a wave filter to remove excess heat or a 150 W high-pressure mercury vapor lamp with a water filter (10 cm) to remove excess heat. In some cases a Schott UG11 filter was used to photolyze in the range 290 nm < λ < 376 nm. Photolysis NMR experiments were carried out in quartz NMR tubes (Wilmad) or in glass tubes fitted with a PTFE stopcock for manipulation under reactive atmospheres. Low temperature photolysis was achieved by passing the gas evaporating from liquid nitrogen through a thermostated dewar, using a 300 W xenon arc lamp as the photolysis source. Photolysis and product characterization in York was achieved by loading the compound into an NMR tube with a PTFE stopcock in a glovebox with an argon atmosphere. Dry solvents were added by cannula, and the sample was degassed by three freeze−pump−thaw cycles before backfilling with the required atmosphere. After photolysis the solvent was removed *in vacuo* before condensing deuterated solvent onto the product mixture. The products were analyzed by ^{1}H and ^{31}P{^{1}H} NMR spectroscopy.

^{1}H and ^{13}C{^{1}H} NMR spectra were recorded on Varian VXR 300, Bruker AC200P, Bruker AVANCE DRX 500, Jeol EX270, or Bruker AMX500 spectrometers operating at 200.13, 270.05, 299.94 or 500.13 MHz (^{1}H) and 50.32, 75.42, and 125.80 MHz (^{13}C). Chemical shifts are given relative to tetramethylsilane and were calibrated against the residual solvent resonance (^{1}H) or the deuterated solvent multiplet (^{13}C). ^{31}P{^{1}H} NMR spectra were measured relative to external 85% H$_3$PO$_4$ with downfield values taken as positive. ^{15}N{^{1}H} NMR spectra were acquired on a Bruker AMX500 and calibrated relative to dissolved ^{15}N$_2$ at δ 309.5. ^{13}C-DEPT experiments were run on the Bruker AC 200P spectrometer. ^{1}H,^{13}C-2D HETCOR NMR experiments were recorded on either the Bruker AC 200P spectrometer using the XHCORR pulse program or the Bruker AVANCE DRX 500 spectrometer equipped with a 5-mm triple resonance probe-head (inverse correlation mode, HMQC experiment). The ^{1}H,^{1}H-2D COSY NMR experiments were conducted routinely on the Bruker AC 200P instrument in the absolute magnitude mode using a 45° or 90° pulse after the incremental delay or were acquired on the AVANCE DRX 500 Bruker spectrometer using the gradient-accelerated version of the conventional COSY sequence (COSYPS). ^{1}H,^{1}H-2D NOESY NMR experiments on **8Os** were conducted on the same instrument operating in the phase-sensitive TPPI mode in order to discriminate between positive and negative cross peaks. The proton NMR spectra, with broadband and selective phosphorus decoupling, were recorded on the Bruker AC 200P instrument equipped with a 5-mm inverse probe and a BFX-5 amplifier device using the decoupling sequence GARP. Infrared spectra were recorded as Nujol mulls or in solution on a Perkin-Elmer 1600 series or a Mattson-Unicam RS FT-IR spectrophotometer between KBr plates. Elemental analyses (C, H, N) were performed using a Carlo Erba Model 1106 elemental analyzer.

NMR data (^{1}H and ^{31}P{^{1}H}) for the complexes synthesized as below are listed in Tables 1 (Ru) and 2 (Os).

Photolysis of Ru(PP$_3$)H$_2$ under Helium. (A) NMR Experiment in THF-*d*$_8$. A solution of **1Ru** (20 mg, 0.026 mmol) in THF-*d*$_8$ (1.0 mL) prepared under helium in a 5-mm NMR quartz tube was irradiated with UV light at 293 K. The photolysis reaction was monitored by ^{31}P{^{1}H} NMR spectroscopy: the cyclometalated complex Ru[(Ph$_2$PCH$_2$-CH$_2$)$_2$P(CH$_2$CH$_2$PPhC$_6$H$_4$)]H (**4Ru**) was the only ruthenium product. After 2 h, ^{31}P{^{1}H} and ^{1}H NMR spectra showed *ca.* 85% conversion of **1Ru** into **4Ru**.

(B) Preparative Experiment in THF. A solution of **1Ru** (200 mg, 0.26 mmol) in THF (20 mL) was irradiated with UV light at 293 K under helium. After 2 h, addition of hexane (30 mL) to the resulting light orange solution led to the precipitation of **4Ru** as pale yellow microcrystals. Yield 75%. Anal. Calcd for C$_{42}$H$_{42}$P$_4$Ru: C, 65.37; H, 5.49. Found: C, 65.21; H, 5.39. IR: ν(Ru−H) 1950 cm^{-1} (m).

Photolysis of Ru(PP$_3$)H$_2$ in Benzene/THF-*d*$_8$. A solution of **1Ru** in C$_6$H$_6$/THF-*d*$_8$ (25:75 v/v) prepared under argon in a 5-mm NMR tube was irradiated with UV light at 243 K for ca 5 h. The sample was kept at 243 K, and low temperature ^{31}P{^{1}H} and ^{1}H NMR spectroscopy (223 K) showed that **1Ru** had disappeared to give a new product Ru(PP$_3$)(Ph)H (**5Ru**). On warming to 273 K, **5Ru** decomposed rapidly to reform **1Ru**, in addition to **4Ru** and other products.

Photolysis of Ru(PP$_3$)H$_2$ under Nitrogen in THF. A solution of **1Ru** (200 mg, 0.26 mmol) in THF (20 mL) was irradiated with UV light at 293 K under nitrogen. After 50 min, a sample of the resulting red orange solution (0.6 mL) was transferred *via* syringe into a 5-mm screw-cap NMR tube containing 0.3 mL of degassed THF-*d*$_8$ and studied by ^{31}P{^{1}H} NMR spectroscopy. The NMR analysis showed the partial conversion (*ca.* 30%) of **1Ru** to Ru(PP$_3$)(N$_2$) (**6Ru**) (see below). Trace amounts of **4Ru** (∼2%) were also detected. After 2 h of photolysis the ^{31}P{^{1}H} NMR analysis gave the following composition: **6Ru** (44%), **4Ru** (8%), **1Ru** (48%).

Synthesis of Ru(PP$_3$)(N$_2$) (6Ru). (A). A solution of sodium naphthalenide prepared in THF (30 mL) from 130 mg (1.04 mmol) of naphthalene and 50 mg of freshly cut sodium (2.20 mmol) was added in small portions with stirring to a THF (10 mL) suspension of Ru-(PP$_3$)Cl$_2$ (**2Ru**) (400 mg, 0.48 mmol) at 273 K. The pale yellow suspension turned red-brown immediately, while the starting dichloride dissolved completely. After stirring for 30 min at 273 K, the ice-bath was removed, and the solution was slowly brought to room temperature and stirred for an additional 30 min. The red-brown solution was filtered and concentrated to about 15 mL under vacuum. Addition of hexane (30 mL) gave red microcrystals of Ru(PP$_3$)(N$_2$) (**6Ru**). Yield 78%. Anal. Calcd for C$_{42}$H$_{42}$N$_2$P$_4$Ru: C, 63.07; H, 5.30; N, 3.50. Found: C, 62.95; H, 5.25; N, 3.31. IR: ν(N≡N) 2080 cm^{-1} (m).

(B). Phenyllithium (0.072 mmol; 40 μL of a solution 1.8 M in diethyl ether−cyclohexane) was syringed into a screw-cap NMR tube containing a solution of [Ru(PP$_3$)(H)(N$_2$)]BPh$_4$ (**3Ru**) (36 mg, 0.033 mmol) in THF-*d*$_8$ (0.8 mL) at 195 K. The yellow solution immediately turned red-brown. The ^{31}P{^{1}H} NMR spectrum showed that **6Ru** was the main product (80%). Two other unidentified products were formed, neither of which contained hydride ligands.

(C). Nitrogen was bubbled into a solution of **4Ru** in THF-*d*$_8$ (1.0 mL) prepared by photolysis of **1Ru** (30 mg, 0.039 mmol) under argon in a 5-mm NMR quartz tube. The reaction was monitored by ^{31}P{^{1}H} NMR spectroscopy which showed the selective formation of **6Ru**. A complete transformation occurred after 24 h in the dark.

Several experiments were carried out to study the thermal behavior of **6Ru** in both THF and C$_6$H$_6$ under either N$_2$ or Ar atmosphere. Extensive decomposition of the compound invariably occurred to unidentified products. In particular, the formation of **4Ru** or **5Ru** was never observed.

Synthesis of Ru(PP$_3$)(CO) (7Ru). A solution of sodium naphthalenide prepared in THF (10 mL) from 65 mg (0.52 mmol) of naphthalene and 25 mg of freshly cut sodium (1.10 mmol) was added in small portions with stirring under a positive pressure of carbon monoxide to a THF solution (8 mL) of **2Ru** (200 mg, 0.24 mol) cooled to 273 K. The pale yellow suspension turned dark yellow immediately while the starting dichloride dissolved. After stirring for 5 min at 273 K, the solution was evaporated to dryness under vacuum to yield a dark yellow solid which was washed with CO-saturated pentane (3 × 5 mL) before being dried under vacuum. Yield 92%. Anal. Calcd for C$_{43}$H$_{42}$OP$_4$Ru: C, 64.58; H, 5.29. Found: C, 64.72; H, 5.11. IR: ν(C≡O) 1866 cm^{-1}.[14] ^{13}C{^{1}H} NMR (295 K, THF-*d*$_8$, 50.32 MHz,

(14) Compare with [Ru(CO)(QP)] (QP = P(*o*-C$_6$H$_4$PPh$_2$)$_3$): ν(C≡O) 1891 cm^{-1}, see: Halfpenny, M. T.; Venanzi, L. M. *Inorg. Chim. Acta* **1971**, *5*, 91.

CO atmosphere in a sealed NMR tube): δ 224.0 (dq, J_{CPb} 72.1 Hz, J_{CPt} 12.0 Hz, Ru*C*O (P_b = bridgehead; P_t = terminal in C_{3v})).[15]

Reduction of $Os(PP_3)Cl_2$ (2Os) with Sodium Naphthalenide. A slight excess of sodium naphthalenide prepared in THF (30 mL) from 130 mg (1.04 mmol) of naphthalene and 50 mg of freshly cut sodium (2.20 mmol) was added in portions with stirring to a suspension of **2Os** (150 mg, 0.16 mmol) in THF (10 mL) thermostated at 273 K under N_2. The starting dichloride dissolved to give a dark red solution. After 15 min, the solution was concentrated in vacuo to give a dark red oil. Due to the extreme air- and moisture-sensitivity of this product neither a satisfactory elemental analysis nor a complete spectroscopic characterization was obtained. However, based on the $^{31}P\{^1H\}$ NMR spectrum (253 K) as well as the chemical behavior (see below) and a comparison with the analogous Ru chemistry, this product was assigned the formula $Os(PP_3)(N_2)$ (**6Os**).

Synthesis of $Os(PP_3)(2\text{-}C_4H_7O)H$ (8Os). On standing at room temperature for 30 min, the red solution of **6Os** obtained as described above, turned orange and, after addition of hexane and concentration under nitrogen, pale orange microcrystals of the (tetrahydrofuranyl)-hydride (**8Os**) separated in about 60% yield. Anal. Calcd for $C_{46}H_{49}P_4OsO$: C, 59.15; H, 5.25. Found: C, 58.89; H, 5.16. IR: ν(Os−H) = 1996 cm^{-1}. $^{13}C\{^1H\}$ NMR (295 K, C_6D_6, 125.77 MHz, assigned by HETCOR) C_4H_7O ring: δ 59.0 (dd, J_{CPtr} 57.1 Hz, J_{CPcis} 10.4 Hz, C_1(P_{tr} = terminal P *trans* to one P in C_s, P_{cis} = terminal P *cis* to all other P in C_s), δ 47.8 (s, C_2), δ 28.2 (s, C_3), δ 71.0 (d, J_{CPtr} 5.2 Hz, C_4). The compound is extremely sensitive to air and moisture and decomposes in THF at 343 K (sealed NMR tube) without formation of any known product.

Photochemical Behavior of 8Os in THF Solution. A solution of **8Os** (40 mg, 0.05 mmol) in THF-d_8 (0.8 mL) was irradiated with UV light in a quartz NMR tube for 90 min at room temperature. $^{31}P\{^1H\}$ and ^1H spectroscopy showed the transformation of **8Os** into the cyclometalated complex $Os[(Ph_2PCH_2CH_2)_2P(CH_2CH_2PPhC_6H_4)]H$ (**4Os**). Decomposition to unidentified products (ca. 20%) was also observed.

Synthesis of the (Phenyl)hydride Complex $Os(PP_3)(Ph)H$ (5Os). (A). A solution of **2Os** (100 mg, 0.12 mmol) in C_6H_6 (15 mL) was stirred for 4 h in the presence of an excess of sodium amalgam (1.5% of Na) under nitrogen. Afterwards, the yellow solution was filtered to remove the amalgam, and the solvent was removed in vacuo to give a solid residue that was characterized as the (phenyl)hydride complex $Os(PP_3)(Ph)H$ (**5Os**) (86%) (IR: ν(Os−H) = 2054 cm^{-1}), occasionally contaminated by the known complex $Os(PP_3)(Cl)H$ (**9Os**).[9]

(B). A solution of **8Os** (40 mg, 0.05 mmol) in C_6D_6 (0.8 mL) in a sealed NMR tube was monitored periodically by $^{31}P\{^1H\}$ NMR spectroscopy at room temperature. After 4 days, all the starting material **8Os** was transformed into $Os(PP_3)(D)(C_6D_5)$ (**5Os-d_6**). **(C)**. A solution of **8Os** (40 mg, 0.05 mmol) in C_6D_6 (0.8 mL) was irradiated with UV light in a quartz NMR tube for 90 min at room temperature. $^{31}P\{^1H\}$ and ^1H spectroscopy showed the complete transformation of **8Os** into **5Os-d_6**.

Synthesis of the (η^1-*O*-Triflate)hydride Complex $Os(PP_3)(OTf)H$ (12Os). A solution of **1Os** (200 mg, 0.23 mmol) in benzene (25 mL) prepared under argon was treated with 1 equiv of MeOTf (26 μL) under vigorous stirring. On evaporation of the solvent under a brisk current of argon, pale yellow needles of $Os(PP_3)(OTf)H$ (**12Os**) separated within a few minutes. Addition of ice-cold hexane previously degassed under argon completed the precipitation of **12Os**. Yield 90%. Anal. Calcd for $C_{43}H_{43}F_3O_3P_4OsS$: C, 51.08; H, 4.29. Found: C, 51.16; H, 4.42. IR: ν(Os−H) 2027 cm^{-1}; $\nu(S-O)_{coord}$ 1314 cm^{-1}.

Reaction of 12Os with MeLi. (A) *In situ* Generation of $Os(PP_3)(CH_3)H$ (13Os). To a solution of **12Os** in C_6D_6 in a 5-mm screw-cap NMR tube at room temperature, 1.25 equiv of MeLi (1.6 mol dm^{-3} solution in Et_2O) were added with a syringe. A $^{31}P\{^1H\}$ NMR spectrum of the resulting light orange solution was recorded immediately. The NMR analysis revealed the quantitative formation of the (methyl)-hydride complex $Os(PP_3)(CH_3)H$ (**13Os**). On standing, $Os(PP_3)(C_6D_5)D$ (**5Os-d_6**) was formed at the expense of **13Os**.

(15) Compare with [(triphos)Ru(CO)$_2$] (triphos = $MeC(CH_2PPh_2)_3$): δ_{RuCO} 221.8 (m), see: Hommeltoft, S. I.; Baird, M. C. *Organometallics* **1986**, *5*, 190. The synthesis of [(triphos)Ru(CO)$_2$] was originally reported by Siegl, W. O.; Lapporte, S. J.; Collman, J. P. *Inorg Chem.* **1973**, *12*, 674.

(B) Preparation of $Os(PP_3)(CH_3)H$ (13Os). A Schlenk tube was charged with 200 mg of **1Os** (0.23 mmol) and 10 mL of benzene previously degassed under argon. After the solution was cooled to *ca.* 279 K, 1 equiv of both MeOTf and MeLi were added via syringe in a quick sequence with stirring. Removal of the solvent *in vacuo* gave a solid residue which was washed with pentane (2 × 3 mL) and characterized as a mixture of **5Os** (45%), **1Os** (25%), **13Os** (25%), and **12Os** (5%) (^{31}P and ^1H NMR integration). IR data for **13Os**: ν(Os−H) 2042 cm^{-1}.

Synthesis of the (Phenyl)hydride Complex $Os(PP_3)(Ph)H$ (5Os) via 12Os. A Schlenk tube was charged with 200 mg of **1Os** (0.23 mmol) and 10 mL of benzene previously degassed under argon. After the solution was cooled to *ca.* 279 K, 1 equiv of both MeOTf (26 μL) and MeLi (145 μL, 1.6 mol dm^{-3} solution in Et_2O) was added via syringe in a quick sequence with stirring. Addition of hexane (5 mL) and slow concentration under argon gave off-white crystals of 5**Os**.Yield 85%.

Results

1. Product Studies of the Photochemical Reactions of $Ru(PP_3)H_2$ and Related Reductive Syntheses. NMR studies of $Ru(PP_3)H_2$ (**1Ru**) show the hydride resonance as a broad doublet in the proton spectrum at δ −6.66. The $^{31}P\{^1H\}$ NMR spectrum reveals the bridgehead phosphorus (P_b) as a quartet at δ 157.0 and the three terminal phosphorus nuclei (P_t) of the tripodal ligand as a doublet at δ 76.7. The fluxional behavior of **1Ru** has been investigated previously.[9] (See Table 1 for details of NMR spectra of complexes of $Ru(PP_3)$.)

A sample of **1Ru** was dissolved in THF and placed under an atmosphere of Research Grade argon. After photolysis for ca. 20 h (290 nm < λ < 376 nm) the $^{31}P\{^1H\}$ NMR spectrum showed a product with an AMQX splitting pattern, and the proton spectrum revealed a new hydride resonance. The same product was made on a preparative scale by taking a solution of **1Ru** in THF and irradiating with UV light at 293 K under helium. The yellow microcrystalline product is identified as the cyclometalated species, $Ru[(Ph_2PCH_2CH_2)_2P(CH_2CH_2\text{-}PPhC_6H_4)]H$ (**4Ru**), on the basis of the large upfield shift (approximately 80 ppm) of one of the phosphorus resonances[16] and the relatively low field resonance of the hydride (Scheme 2). This complex reacted thermally under 1 atm of hydrogen to reform **1Ru** within a few minutes (Scheme 3), behavior which is similar to that of $Fe(Ph_2PCH_2CH_2PPh_2)(C_6H_4PPhCH_2CH_2\text{-}PPh_2)H$ with H_2.[17]

The cyclometalated complex (**4Ru**) also reacts thermally with nitrogen (1 atm) at ambient temperature to form the dinitrogen complex, $Ru(PP_3)(N_2)$ (**6Ru**) (Scheme 3). $Ru(PP_3)(N_2)$ was generated by several other means: (i) by direct photolysis of **1Ru** in THF under N_2, giving **6Ru** and **4Ru** in 40% and 25% yields, respectively (Scheme 2); (ii) by the addition of sodium naphthalenide to a solution of $Ru(PP_3)Cl_2$ (**2Ru**) under an N_2 atmosphere; and (iii) by adding phenyllithium to a solution of $[Ru(PP_3)(H)(N_2)]BPh_4$ (**3Ru**) in THF-d_8 at 195 K (Scheme 4). $Ru(PP_3)(N_2)$ is a red crystalline complex ($\nu(N{\equiv}N)$ = 2080 cm^{-1}; λ_{max} = 410 nm) which was fully characterized by $^{31}P\text{-}\{^1H\}$ and ^1H NMR. The $^{31}P\{^1H\}$ NMR spectrum (Figure 1a) shows an AM_3 pattern with a large P−P coupling (23.5 Hz). In addition, the labeled complex, $Ru(PP_3)(^{15}N_2)$ (**6Ru-$^{15}N_2$**) was formed by photolysis. The $^{31}P\{^1H\}$ spectrum displayed the extra couplings to two ^{15}N nuclei (Figure 1b). The $^{15}N\{^1H\}$ spectrum showed three resonances. A large sharp singlet at δ 309.5 is assigned to $^{15}N_2$ gas in solution. The inequivalent ^{15}N nuclei of **6Ru-$^{15}N_2$** appear as a doublet of quintets at δ 317.9 and a broad peak at δ 356.7 (Figure 1c). These splitting patterns confirm the structure as the η^1-N_2 complex. Previous $^{15}N\{^1H\}$ NMR data for dinitrogen complexes are sparse. However,

(16) Garrou, P. E. *Chem. Rev.* **1981**, *81*, 229.
(17) Azizian, H.; Morris, R. H. *Inorg. Chem.* **1983**, *22*, 6.

Table 1. Selected ^{1}H, ^{15}N{^{1}H}, and ^{31}P{^{1}H}NMR Data for the Ru(PP$_3$)L and Ru(PP$_3$)(X)H compounds[e,f]

complex	nucleus	δ/ppm	coupling constant, J/Hz		assignment
Ru(PP$_3$)H$_2$	^{1}H[a]	−6.66	br d	fluxional	hydride
1Ru	^{31}P[a]	157.0	q	J(P$_t$) 7.2	P$_b$
		76.7	d	J(P$_b$) 7.0	P$_t$
cyclometalated	^{1}H[b]	−0.25	dq	J(P$_b$) 80.5, J(P$_{cy}$, P$_{cis}$, P$_{tr}$) 17.5	hydride
complex	^{31}P[b]	145.0	dd	J(P$_{cy}$) 9.7, J(P$_{tr}$) 6.2	P$_b$
4Ru		83.7	ddd	J(P$_{cy}$) 275.7, J(P$_{cis}$) 15.2, J(P$_b$) 6.1	P$_{tr}$
		76.6	dd	J(P$_{tr}$) 15.2, J(P$_{cy}$) 24.3	P$_{cis}$
		−7.7	ddd	J(P$_{tr}$) 275.0, J(P$_{cis}$) 24.3, J(P$_b$) 9.4	P$_{cy}$
Ru(PP$_3$)(Ph)H	^{1}H[a]	−8.22	br d	fluxional	hydride
(300 K)	^{31}P[a]	142.9	q	J(P$_t$) 9.2	P$_b$
5Ru		59.4	br	fluxional	P$_t$
		49.7	br	fluxional	P$_t$
Ru(PP$_3$)(Ph)H	^{1}H[c]	−8.22	dtd	J(P$_{cis}$) 81.2, J(P$_{tr}$) 24.7, J(P$_b$) 12.9	hydride
(273 K)	^{31}P[c]	141.1	td	J(P$_{tr}$) 11.3, J(P$_{cis}$) 2.2	P$_b$
5Ru		55.7	ps t	J(P$_b$, P$_{cis}$) 11.8	P$_{tr}$
		47.4	td	J(P$_{tr}$) 11.6, J(P$_b$) 2.1	P$_{cis}$
Ru(PP$_3$)(^{14}N$_2$)	^{31}P[b]	159.4	q	J(P$_t$) 23.5	P$_b$
6Ru		69.4	d	J(P$_b$) 23.5	P$_t$
Ru(PP$_3$)(^{15}N$_2$)	^{31}P[b]	159.5	dqd	J(N$_\alpha$) 29.8, J(P$_t$) 23.6, J(N$_\beta$) 2.2	P$_b$
6Ru-^{15}N$_2$		69.4	ddd	J(P$_b$) 23.6, J(N$_\alpha$) 4.8, J(N$_\beta$) 1.8	P$_t$
	^{15}N[b]	317.9	dquin	J(P$_b$) 29.4, J(P$_t$, N$_\beta$) 4.7	N$_\alpha$
		356.7	br		N$_\beta$
Ru(PP$_3$)(CO)	^{31}P[a]	163.7	q	J(P$_t$) 30.5	P$_b$
7Ru		79.5	d	J(P$_b$) 30.5	P$_t$
Ru(PP$_3$)(Cl)H	^{1}H[a]	−7.95	dq	J(P$_b$) 96.8, J(P$_{tr}$, P$_{cis}$) 23.8	hydride
9Ru	^{31}P[a]	150.2	td	J(P$_{tr}$) 14.1, J(P$_{cis}$) 6.8	P$_b$
		48.3	ps t	J(P$_b$, P$_{cis}$) 14.2	P$_{tr}$
		38.4	td	J(P$_{tr}$) 14.6, J(P$_b$) 6.9	P$_{cis}$
Ru(PP$_3$)(C$_2$H$_4$)	^{1}H[a]	2.49	dq	J(P$_b$) 3.8, J(P$_t$) 0.8	C$_2$H$_4$
10Ru	^{31}P[a]	160.9	q	J(P$_t$) 30.0	P$_b$
		73.9	d	J(P$_b$) 30.0	P$_t$
Ru(PP$_3$)(SiEt$_3$)H	^{1}H[b]	−9.77	dq[d]	J(P$_b$) 8.8, J(P$_{tr}$, P$_{cis}$) 5.4, fluxional	hydride
(300 K)		0.74	t	J(Si(C*H*$_2$CH$_3$)$_3$) 7.5	silyl C*H*$_3$'s
11Ru		0.82	q	J(Si(CH$_2$C*H*$_3$)$_3$) 7.5	silyl C*H*$_2$'s
	^{31}P[b]	153.2	q	J(P$_t$) 14.7	P$_b$
		69.7	d	J(P$_b$) 14.6	P$_t$
Ru(PP$_3$)(SiEt$_3$)H	^{1}H[b]	−9.63	dtd[d]	J(P$_{cis}$) 66.7, J(P$_{tr}$) 24.8, J(P$_b$) 7.8	hydride
(175 K)	^{31}P[b]	156.9	br		P$_b$
11Ru		75.9	br		P$_{tr}$ or P$_{cis}$
		70.7	br		P$_{tr}$ or P$_{cis}$

[a] In C$_6$D$_6$. [b] In THF-d_8. [c] In 3:1 mixture THF-d_8: C$_6$H$_6$. [d] See text for comments on signs of coupling constants. [e] Key to subscripts: P$_b$ = bridgehead; P$_t$ = terminal (in C_{3v}); P$_{cis}$ = terminal P *cis* to all other P in C_s; P$_{tr}$ = terminal P *trans* to one P in C_s; P$_{cy}$ = cyclometalated P; N$_\alpha$ = nitrogen attached to metal center; N$_\beta$ = nitrogen furthest away from metal center. [f] ^{1}H NMR data for the PP$_3$ ligands excluded.

RhCl(N$_2$)(PPr$^i_3$)$_2$ shows similar shifts and couplings to **6Ru-^{15}N$_2$**.[18] Like the cyclometalated complex (**4Ru**), **6Ru** reacts thermally with H$_2$ at room temperature, to form **1Ru** over a few minutes (Scheme 3). Experiments designed to study the thermal behavior of **6Ru** in THF under either N$_2$ or Ar atmosphere invariably resulted in decomposition. Photolysis of **1Ru** in THF under argon atmospheres containing only trace amounts of N$_2$ (BOC Pureshield Argon, 99.995%) still yields **6Ru** in small amounts. At such low concentrations this must be attributed to the efficient scavenging of N$_2$ by the cyclometalated complex (**4Ru**).

Photolysis of **1Ru** in a large volume of hexane under an atmosphere of CO for 1 h resulted in the formation of a product which showed an AM$_3$ pattern in the ^{31}P{^{1}H} NMR spectrum and a large coupling constant (J_{PP} = 30.5 Hz) suggestive of a Ru(0) product with local C_{3v} symmetry. A doublet of quartets at δ 224.0 in the ^{13}C{^{1}H} NMR spectrum assigned to the carbonyl carbon atom confirms the trigonal bipyramidal structure of Ru(PP$_3$)(CO) (**7Ru**, IR, hexane: ν(CO) = 1890 cm^{-1}, UV/visible: λ_{max} = 380 nm). Complex **7Ru** could be made on a preparative scale by reduction of **2Ru** in the presence of carbon monoxide (Scheme 4).

When **1Ru** was photolyzed for 5 h in a 3:1 (v/v) mixture of THF-d_8 and C$_6$H$_6$ at 243 K, low temperature ^{31}P{^{1}H} NMR spectra of the resulting orange-yellow solution showed selective formation of Ru(PP$_3$)(Ph)H (**5Ru**) (Scheme 2). The ^{1}H NMR spectrum of **5Ru** at 233 K exhibited a hydride resonance at δ −8.22 with a doublet of triplets of doublets splitting, while the ^{31}P{^{1}H} NMR showed three broad triplets. At higher temperatures (273 K) the ^{31}P{^{1}H} NMR spectrum sharpened to give a triplet of doublets at δ 141.1, a pseudo triplet at δ 55.7 and a triplet of doublets at δ 47.4, which is a characteristic AMQ$_2$ pattern. The stereochemistry of **5Ru** was determined by selective phosphorus decoupling of the ^{1}H NMR spectrum. This revealed that the hydride was *trans* to P$_{cis}$, with the large *trans* coupling destroyed by irradiation at δ 47.4. As the solution is warmed to 293 K, **5Ru** reacts with expelled H$_2$ to reform **1Ru**; formation of **4Ru** together with small amounts of a new species is also observed.

In contrast to the low temperature experiments, photolysis of **1Ru** in benzene (AR Grade) under an atmosphere of argon (99.995%) at room temperature led to a mixture of products by ^{31}P{^{1}H} and ^{1}H NMR analysis, in which the major product was identified as **4Ru**. When Ru(PP$_3$)Cl$_2$ (**2Ru**) was stirred with a Na/Hg amalgam in benzene at room temperature, a mixture of **5Ru** and **4Ru** were formed (Scheme 5). On placing this mixture under nitrogen the products were converted to Ru(PP$_3$)(N$_2$) (**6Ru**). Conversely, **5Ru** could not be formed by thermal reaction of **6Ru** with benzene.

A sample of **1Ru** in toluene was photolyzed (90 min) under an atmosphere of ethene and redissolved in C$_6$D$_6$. The ^{31}P{^{1}H} NMR spectrum featured an AM$_3$ pattern with a large coupling

Scheme 2. Photochemical Reactions of $Ru(PP_3)H_2$

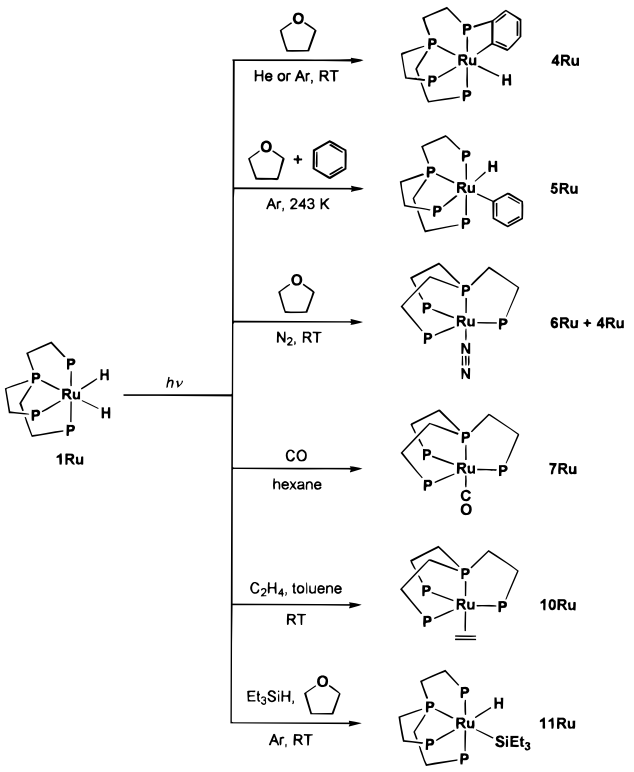

Scheme 3. Reactions of the Cyclometalated $Ru(PP_3)$

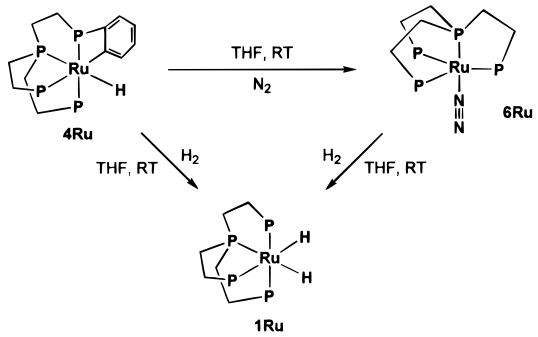

constant (J_{PP} = 30.0 Hz), which is typical of a C_{3v} Ru(0) species. The ^{1}H NMR spectrum showed a doublet of quartets which collapsed to a singlet on selective phosphorus decoupling. This resonance is assigned to four equiv ethene protons coupled to the unique apical phosphorus and the three equiv terminal phosphorus donor atoms. The product is assigned as the η^2-ethene complex (**10Ru**) (Scheme 2). No attempt was made to isolate the product.

A sample of **1Ru** dissolved in a 2:1 (v/v) mixture of THF-d_8 and $HSiEt_3$ was photolyzed for 2 h. The resulting solution was evaporated to dryness, washed with hexane (to remove involatile organosilanes), and redissolved in THF-d_8. The ^{1}H NMR spectrum at 175 K showed a hydride resonance as a doublet of triplets of doublets, and the $^{31}P\{^1H\}$ NMR spectrum exhibited three broad resonances. The product is assigned as the silyl hydride complex, $Ru(PP_3)(SiEt_3)H$ (**11Ru**). Selective phosphorus decoupling of the ^{1}H NMR spectrum revealed that the hydride ligand of **11Ru** is *trans* to P_{cis}. Complex **11Ru** proved to be highly fluxional. At room temperature, the $^{31}P\{^1H\}$ NMR spectrum showed an AM_3 pattern, and the ^{1}H spectrum showed a doublet of quartets for the hydride resonance. The hydride couplings to P_{cis} and P_{tr} for **11Ru** at room temperature (J_{PH} = 8.8, 5.4 Hz) agree with the average of those at 175 K, provided that the coupling $J(P_{cis})$ is taken as the opposite sign of $J(P_{tr})$.

2. Product Studies of the Photochemical Reactions of Os-

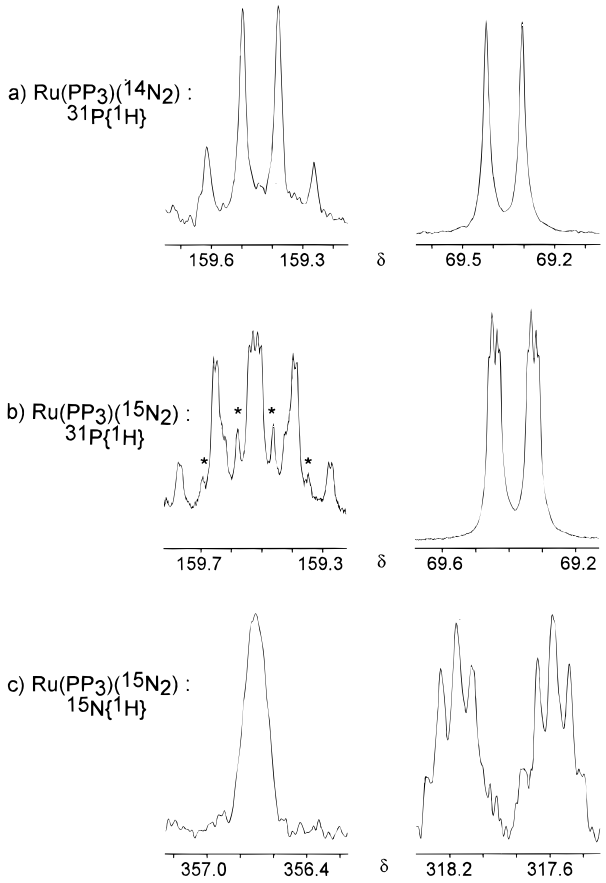

Figure 1. (a) $^{31}P\{^1H\}$ NMR spectrum of $Ru(PP_3)(^{14}N_2)$; (b) $^{31}P\{^1H\}$ NMR spectrum of $Ru(PP_3)(^{15}N_2)$; and (c) $^{15}N\{^1H\}$ NMR spectrum of $Ru(PP_3)(^{15}N_2)$. Resonances marked * due to residual $Ru(PP_3)(^{14}N_2)$.

Scheme 4. Thermal Routes to $Ru(PP_3)(N_2)$ and $Ru(PP_3)(CO)$

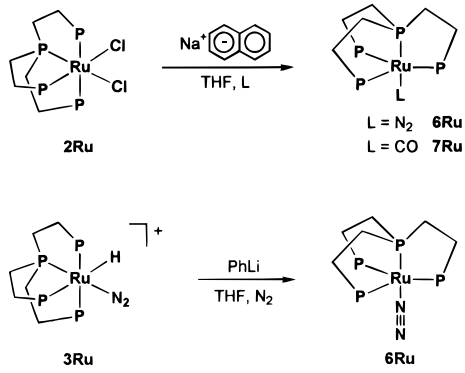

$(PP_3)H_2$ and Related Syntheses. The ^{1}H NMR spectrum of $Os(PP_3)H_2$ (**1Os**) shows a broad hydride resonance at δ −7.85. The $^{31}P\{^1H\}$ NMR spectrum shows an AM_3 pattern with a quartet at δ 134.8 (J = 5.0 Hz) and a doublet at δ 45.8 (J = 4.9 Hz). These observations indicate that the dihydride is fluxional (cf. $Ru(PP_3)H_2$).[10] The NMR data for complexes of $Os(PP_3)$ are listed in Table 2.

A sample of **1Os** in benzene solution was photolyzed for 1 h (290 nm < λ < 376 nm). The ^{1}H NMR spectrum of the product showed a doublet of triplets of doublets in the hydride region and new multiplets in the aromatic region which integrated in the ratio 1:2:2 relative to the hydride resonance. The $^{31}P\{^1H\}$ NMR spectrum can be analyzed in terms of an AMQ_2 pattern with some unresolvable couplings. The product of the reaction can therefore be identified as $Os(PP_3)(Ph)H$ (**5Os**) (Scheme 6). Confirmation is obtained by synthesis of the compound via reduction of $Os(PP_3)Cl_2$ (**2Os**) in benzene with Na/Hg amalgam (Scheme 7).

Scheme 5. Thermal Synthesis of Ru(PP$_3$)(Ph)H

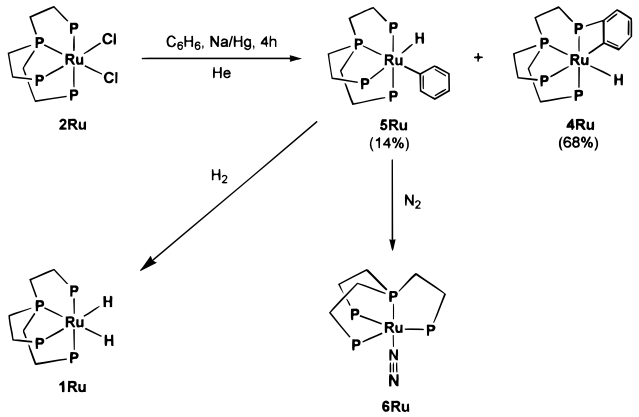

Products of the photolysis of **1Os** in alkane solvents proved unsuitable for analysis by NMR as the solubilities were poor, and hence concentrations of the product were too low. The photolysis of **1Os** for 1.5 h in hexane/THF (3:2 v/v) was attempted in order to overcome low solubility in alkane and give the alkane activated product in yields suitable for NMR analysis. The $^{31}P\{^1H\}$ NMR spectrum showed an AMNQ pattern, with the resonances assigned to the two *trans* phosphorus atoms appearing as a second-order quartet. The ^1H NMR spectrum showed a new hydride resonance coupled to two inequivalent phosphorus nuclei (P_b and P_{cis}) and equally coupled to the two inequivalent *trans* phosphorus nuclei (P_{tr}) leading to a doublet of triplets of doublets. Photolysis in THF alone for about 2 h yielded the same product as that observed in a hexane/THF mixture, while photolysis in THF-d_8 yielded the same product, except that there is no hydride resonance and the resonance assigned to P_{cis} is broadened. This product is assigned not as the alkyl hydride complex as hoped, nor as the cyclometalated product (**4Os**) as described previously,[13] but as the tetrahydrofuranyl hydride complex, Os(PP$_3$)(2-C$_4$H$_7$O)H (**8Os**) (Scheme 6). In addition, **8Os** has been synthesized by reducing Os(PP$_3$)Cl$_2$ (**2Os**) with sodium naphthalenide at 273 K under N_2 and leaving the red product (see below) to stand in THF solution for a short period at room temperature to give orange microcrystals. The compound is extremely air and moisture sensitive and decomposes thermally (343 K). The effect of deuteration allows us to determine the stereochemistry: the hydride must be *trans* to P_{cis} and the tetrahydrofuranyl ring *trans* to the bridgehead phosphorus. A combination of COSY and NOESY spectra of the purified compound allows full assignment of the stereochemistry of the tetrahydrofuranyl ring (Figure 2, Scheme 6).

Prolonged photolysis (ca. 15 h) of **1Os** in THF solution destroyed **8Os** and yielded a new product which shows four resonances in the $^{31}P\{^1H\}$ NMR spectrum, including one which was shifted upfield by about 80 ppm from the terminal resonances in **1Os**. In addition the ^1H NMR spectrum showed a new hydride resonance at relatively low field, δ −2.03. These two factors allow assignment of this product as the cyclometalated complex (**4Os**) (see comments for reaction of Ru(PP$_3$)H$_2$ with THF). Selective phosphorus decoupling showed that the hydride is *trans* to the bridgehead phosphorus in this complex. Thermal and photochemical experiments on purified **8Os** show that the conversion to **4Os** only occurs photochemically (Scheme 8).

The solubility of **1Os** in alkanes is too low for study by NMR spectroscopy. Therefore, the methyl hydride complex, Os(PP$_3$)(Me)H (**13Os**), was synthesized from **1Os** via the triflate hydride complex, Os(PP$_3$)(OTf)H (**12Os**) (Scheme 7). Addition of methyl triflate to a benzene solution of **1Os** yielded pale yellow needles of **12Os**. When MeLi was added immediately after the MeOTf to a C_6D_6 solution of **1Os**, the solution became light orange. A $^{31}P\{^1H\}$ NMR spectrum of the solution revealed the quantitative formation of **13Os**. The solution was left to stand, and $^{31}P\{^1H\}$ NMR spectra showed the conversion of **13Os** to **5Os-d_6** by reductive elimination of methane and reaction with solvent (Scheme 7).

Photolysis of **1Os** in THF under an ethene atmosphere gave a new species in high yield. The ^1H NMR spectrum showed no resonances due to a new hydride, while the $^{31}P\{^1H\}$ NMR spectrum showed a product with an AM_3 splitting pattern. This product can be assigned as the η^2-ethene complex (**10Os**) which is fluxional, hence making the three terminal phosphorus atoms equivalent (Scheme 6).

Addition of sodium naphthalenide to Os(PP$_3$)Cl$_2$ (**2Os**) in THF at 273 K under a N_2 atmosphere yielded an extremely air and moisture sensitive red oil, which was provisionally characterized by $^{31}P\{^1H\}$ NMR as Os(PP$_3$)(N$_2$) (**6Os**) (Scheme 7). However, photolysis of **1Os** under a N_2 atmosphere did not generate **6Os**. Solutions of the phenyl hydride (**5Os**) and cyclometalated complexes (**4Os**) did not convert thermally or photochemically to **6Os** under an atmosphere of N_2 (in contrast with the behavior of the Ru analogues).

3. Transient Photochemistry of Ru(PP$_3$)H$_2$. Ru(PP$_3$)H$_2$ (**1Ru**) is a pale yellow solid; its UV/visible spectrum shows an absorption which increases into the UV with a resolved shoulder at 335 nm in cyclohexane (333 nm in THF). At the laser wavelength of 308 nm, it has an extinction coefficient of 7300 dm^3 mol^{-1} cm^{-1} (THF solution). It is only slightly soluble in cyclohexane but dissolves readily in THF.

Laser flash photolysis of samples of **1Ru** in cyclohexane solution (ca. 10^{-4} mol dm^{-3}) under an atmosphere of H_2 (in order to ensure reversibility) generated a transient within the risetime of the apparatus (ca. 100 ns). The transient showed a broad maximum centered at 395 nm (Figure 3) with no other absorption maxima out to 900 nm. The absorption maximum was shifted to 390 nm on changing the solvent to pentane (also under H_2). All subsequent data were recorded at 400 nm unless otherwise stated.

In cyclohexane solution under an argon atmosphere, the transient signal decayed over several milliseconds and did not return to the baseline, indicating the formation of a longer-lived photoproduct. The decay fitted a plot of ln ΔA against time and gave a first-order rate constant of 350 s^{-1}.[19] In heptane solution under an argon atmosphere, the behavior was similar but the rate constant increased to 610 s^{-1}.

Laser flash photolysis of **1Ru** in cyclohexane was carried out under varying pressures of H_2 (200−760 Torr), always made up to ca. 1 atm with argon (Figure 4). The decay now returned to the baseline with pseudo-first-order kinetics in hundreds of microseconds, an observation consistent with a reaction which reverses thermally. A plot of k_{obs} against [H_2] yielded a straight line and a second-order rate constant of (2.0 ± 0.4) × 10^6 dm^3 mol^{-1} s^{-1} (Table 3, Figure S1 in Supporting Information). A similar rate constant was obtained with hydrogen in pentane. Addition of benzene (0.1−1.5 mol dm^{-3}) to cyclohexane solutions under argon of **1Ru** quenched the transient, but the signal did not return completely to the baseline. A plot of k_{obs} against [benzene] is linear (Table 3, Figure 5). The experiments were repeated with benzene-d_6 (0.09−0.74 mol dm^{-3}) and yielded a kinetic isotope effect, k_H/k_D = 1.5 ± 0.2 (Tables 3 and 4, Figure 5).[20] The quenching kinetics with triethylsilane (0.01−0.06 mol dm^{-3}) in cyclohexane solutions of **1Ru** gave a second-order rate constant, k_2 = (5.4 ± 1.1) × 10^5 dm^3 mol^{-1} s^{-1} (Table 3).

Flash photolysis in the presence of THF (0.008−0.068 mol dm^{-3}) yielded an instantaneous rise when monitored at 470 nm,

Table 2. Selected ^{1}H and ^{31}P{^{1}H} NMR Data for Os(PP$_3$)L and Os(PP$_3$)(X)H Complexes

complex	nucleus	δ/ppm	coupling constant, J/Hz		assignment
$Os(PP_3)H_2$	$^1H^a$	−7.85	br	fluxional	hydride
1Os	$^{31}P^a$	134.8	q	$J(P_t)$ 5.0	P_b
		45.7	d	$J(P_b)$ 4.9	P_t
cyclometalated	$^1H^b$	−2.03	dq	$J(P_b)$ 58, $J(P_{tr}, P_{cis}, P_{cy})$ 14	hydride
complex	$^{31}P^b$	128.4	dd	$J(P_{tr})$ 9, $J(P_{cis})$ 10	P_b
4Os		53.6	ddd	$J(P_{cy})$ 258, $J(P_b)$ 9, $J(P_{cis})$ 4	P_{tr}
		50.6	ddd	$J(P_{cy})$ 19, $J(P_b)$ 10, $J(P_{tr})$ 4	P_{cis}
		−36.4	dd	$J(P_{tr})$ 258, $J(P_{cis})$ 9	P_{cy}
Os(PP$_3$)(Ph)H	$^1H^a$	−8.68	dtd	$J(P_{cis})$ 67.8, $J(P_{tr})$ 29.4, $J(P_b)$ 8.7	hydride
5Os		8.41	m		phenyl
		7.89	m		phenyl
		6.58	m		phenyl
	$^{31}P^a$	122.1	d	$J(P_{cis})$ 9.0	P_b
		25.8	dt	$J(P_b)$ 9.0, $J(P_{tr})$ 4.5	P_{cis}
		23.9	d	$J(P_{cis})$ 4.5	P_{tr}
Os(PP$_3$)(N$_2$)	$^{31}P^c$	136.9	q	$J(P_t)$ 12.1	P_b
6Os		39.2	d	$J(P_b)$ 12.1	P_t
Os(PP$_3$)(2-C$_4$H$_7$O)H	$^1H^b$	−9.12	dtd	$J(P_{cis})$ 65.5, $J(P_{tr})$ 28.9, $J(P_b)$ 8.3	hydride
8Os		6.17	m		H1
		2.55	m		H2
		2.80	m		H3
		2.05	m	second order, masked by PP$_3$ ligand	H4, H5
		3.92	td	J(H6−H7) 7.8	H6
		4.32	td	J(H6−H7) 7.8	H7
	$^{31}P^b$	123.6	ddd	$J(P_{cis})$ 10.6, $J(P_{tr1})$ 2.0, $J(P_{tr2})$ 3.3	P_b
		31.0	ddd	$J(P_{tr2})$ 243.1, $J(P_{cis})$ 6.0, $J(P_b)$ 2.0	P_{tr1}
		28.1	ddd	$J(P_{tr1})$ 243.1, $J(P_{cis})$ 6.0, $J(P_b)$ 3.3	P_{tr2}
		23.0	dt	$J(P_b)$ 10.6, $J(P_{tr1},P_{tr2})$ 6.0	P_{cis}
Os(PP$_3$)(C$_2$H$_4$)	$^{31}P^b$	140.2	q	$J(P_t)$ 12.1	P_b
10Os		42.4	d	$J(P_b)$ 12.9	P_t
Os(PP$_3$)(OTf)H	$^1H^a$	−5.82	dtd	$J(P_{cis})$ 74.5, $J(P_{tr})$ 25.3, $J(P_b)$ 13.6	hydride
12Os	$^{31}P^a$	104.1	dt	$J(P_{cis})$ 8.3, $J(P_{tr})$ 4.2	P_b
		30.1	dt	$J(P_b)$ 8.3, $J(P_{tr})$ 5.7	P_{cis}
		26.9	dd	$J(P_{cis})$ 5.7, $J(P_b)$ 4.2	P_{tr}
Os(PP$_3$)(CH$_3$)H	$^1H^a$	−9.37	dtd	$J(P_{cis})$ 68.3, $J(P_{tr})$ 28.3, $J(P_b)$ 9.1	hydride
13Os		1.24	dq	$J(P_b)$ 18.8, $J(P_{cis}, P_{tr})$ 7.5	methyl
	$^{31}P^a$	127.4	d	$J(P_{cis})$ 8.6	P_b
		26.7	d	$J(P_{cis})$ 6.4	P_{tr}
		20.3	dt	$J(P_b)$ 8.6, $J(P_{tr})$ 6.4	P_{cis}

[a,b]Key to subscripts and superscripts as Table 1. [c] In THF-d_8 at 253 K.

Scheme 6. Photochemical Reactions of Os(PP$_3$)H$_2$

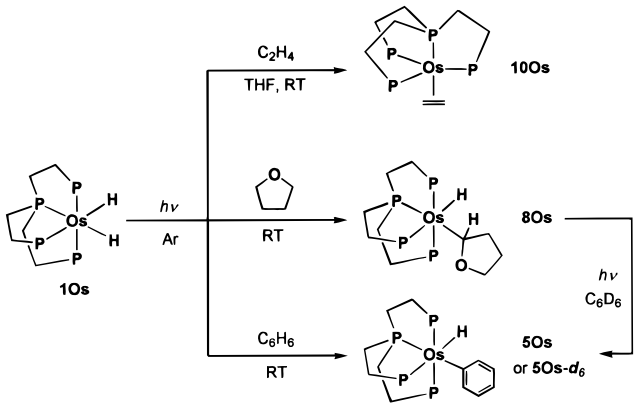

Scheme 7. Thermal Syntheses with Os(PP$_3$)Cl$_2$ and Os(PP$_3$)H$_2$

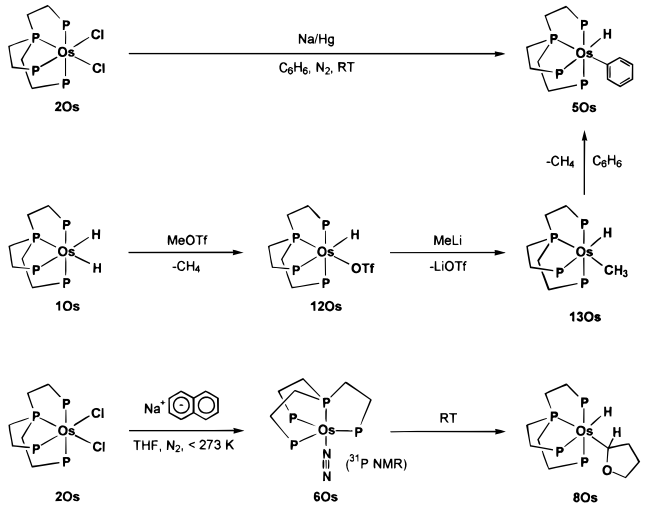

followed by a further rise over tens of microseconds (Figure 6a). This growth showed a linear dependence on THF concentration (Table 3, Figure 6c). The resulting photoproduct (λ_{max} 435 nm) decayed over a few milliseconds (Figure 6b), with a rate constant which showed an inverse dependence on the THF concentration (Figure 6d). The reactions were repeated with THF-d_8 (0.003−0.054 mol dm^{-3}) and identical behavior was observed (Table 3). The kinetic isotope effect proved insignificant (Table 4). The lifetime of the photoproduct is extended to approximately 200 ms in pure THF (12.3 mol dm^{-3}).

The rate of reaction of the transient with CO was determined under varying pressures of CO (10−650 Torr) made up to a total pressure of ca. 1 atm with argon. The transient decayed with pseudo-first-order kinetics, but a long-lived photoproduct absorbed strongly at the usual monitoring wavelength. By monitoring the solutions at 440 nm, decay signals were obtained with minimum product absorption and maximum decay amplitude (cf. λ_{max} for Ru(PP$_3$)(CO) = 380 nm). A plot of observed rate constant against CO concentration is linear (Figure S1, Table 3). As a test for a spin triplet state for the transient, a sample was prepared under 11 Torr of CO filled to 1 atm with

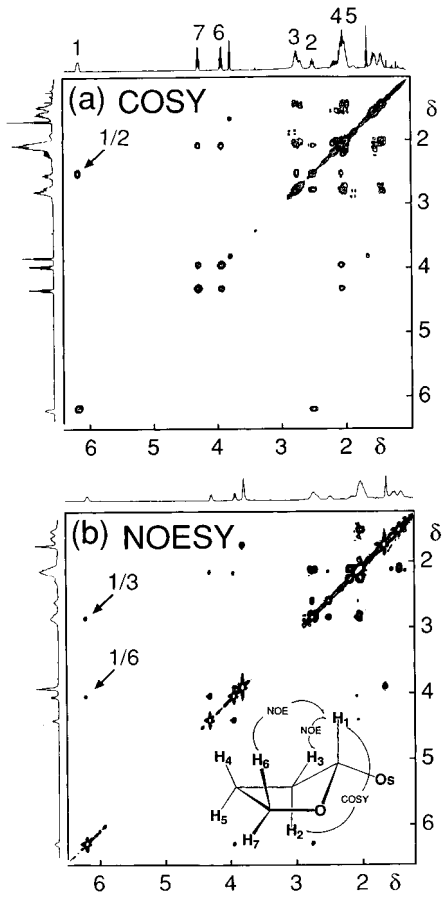

Figure 2. (a) Contour plot of a section of the ^{1}H,^{1}H-COSY spectrum of Os(PP$_3$)(2-C$_4$H$_7$O)H showing the scalar couplings for the protons of the tetrahydrofuranyl ring. The relevant cross-peak between protons H$_1$ and H$_2$ is marked. (b) Section of the phase sensitive ^{1}H,^{1}H-NOESY spectrum (with both positive and negative contours shown) of Os(PP$_3$)-(2-C$_4$H$_7$O)H, showing the spatial relationships between the protons of the tetrahydrofuranyl ring. The relevant negative cross peaks pertaining to the H$_1$ proton are marked. Note that resonances due to the phosphine alkyl backbone are also present in this region.

Scheme 8. Reactions of Os(PP$_3$)(2-C$_4$H$_7$O)H

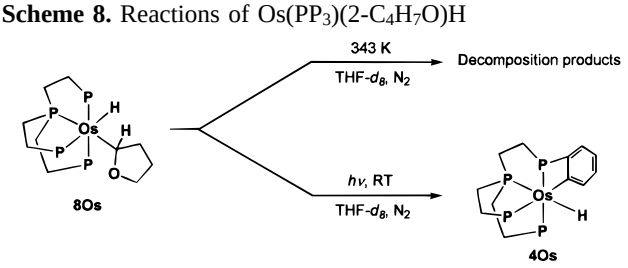

Xe rather than Ar. Xe has a significantly higher solubility[21] than Ar, and its heavy atom effect should assist in overcoming the spin selection rules. However, the rate constants for reaction with CO in the presence of Ar and Xe were not significantly different.

(18) Thorn, D. L.; Tulip, T. H.; Ibers, J. A. *J. Chem. Soc., Dalton Trans.* **1979**, 2022.

(19) The experiment was repeated in cyclohexane-d_{12}, and the pseudo-first-order rate constant was determined as $k_{obs} = 550$ s^{-1}, yielding a kinetic isotope effect of 0.6. Assuming cyclohexene-d_{10} reacts with a similar rate constant to ethene ($k_2 \approx 5 \times 10^5$ dm^3 mol^{-1} s^{-1}), the rate increase can also be accounted for by small amounts of cyclohexene-d_{10} (1 mM) impurity in the cyclohexane-d_{12}. Consequently we do not place any emphasis on this result.

(20) Similar arguments regarding cyclohexene-d_{10} impurities were considered as for Ru(PP$_3$)H$_2$,[19] but the observed rate constant was an order of magnitude greater than expected for quenching by 1 mM cyclohexene-d_{10}, derived on the basis of the rate constant for reaction with ethene and heptene. Consequently we believe that the observed kinetic isotope effect is reliable.

(21) Wilhelm, E.; Battino, R. *Chem. Rev.* **1973**, *73*, 1.

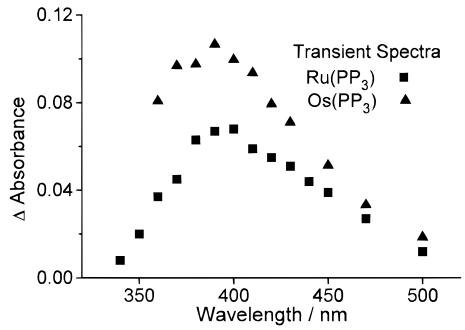

Figure 3. (a) Transient spectrum recorded 10 μs after the laser flash photolysis of Ru(PP$_3$)H$_2$ in cyclohexane (■). (b) Transient spectrum recorded 13 μs after the laser flash photolysis of Os(PP$_3$)H$_2$ in cyclohexane (▲). The spectra were recorded under atmospheres of H$_2$.

The reactivity of the transient with ethene was investigated, and a long-lived photoproduct was observed which absorbed strongly at 400 nm as with quenching by CO. Even at 440 nm the difference in extinction coefficients between the transient and photoproduct was low, but small amplitude decays were obtained at three different partial pressures (Table 3). The reactivity of the transient toward nitrogen (60−770 Torr) was monitored in a similar way. Flash photolysis generated a transient which decayed with pseudo-first-order kinetics to a photoproduct which absorbed very strongly at 400 nm (cf. λ_{max} for Ru(PP$_3$)(N$_2$) = 410 nm). Kinetic measurements were made at 390 nm (Figure S1, Table 3).

Reactivity toward methane was investigated with two samples side-by-side of **1Ru** in cyclohexane, under argon and methane, respectively. The transients produced on flash photolysis decayed with identical rates.

The temperature dependences of the rate constants for the decay of the transient in cyclohexane in the presence of HSiEt$_3$ (0.013 to 0.018 mol dm^{-3}) and benzene (0.15 mol dm^{-3}) were studied from 285−338 and 280−327 K, respectively. Eyring plots of ln(k_2/T) against 1/T yielded straight lines (Table S1, Figure 7). From these plots the activation parameters were determined (Table 5).

The transient observed on laser flash photolysis is readily assigned as Ru(PP$_3$) on consideration of (i) the regeneration of **1Ru** under H$_2$, (ii) the quenching behavior with simple substrates, and (iii) the consistency with the NMR studies of the photochemistry. The transient behavior is summarized by Scheme 9 for all substrates except THF. The more complex behavior on laser flash photolysis of **1Ru** in the presence of THF may be understood through Scheme 10a, where Ru(PP$_3$) reacts reversibly to form Ru(PP$_3$)(OC$_4$H$_8$), which acts as a temporary sink. Meanwhile Ru(PP$_3$) is converted irreversibly to the cyclometalated complex (**4Ru**). Both Ru(PP$_3$) and Ru-(PP$_3$)(OC$_4$H$_8$) contribute to the transient absorption, but the latter has λ_{max} at much longer wavelength (435 nm). Figure 6 represents a fit to this scheme. Although we have no direct evidence, we surmise that the product of photolysis of **1Ru** in pure alkanes is the cyclometalated complex (**4Ru**).

4. Transient Photochemistry of Os(PP$_3$)H$_2$. Os(PP$_3$)H$_2$ (**1Os**) is a creamy-white solid; its UV/visible spectrum shows no visible absorption maximum but an absorption which increases into the UV region with a shoulder at 310 nm. It has an extinction coefficient of 4600 dm^3 mol^{-1} cm^{-1} at the laser wavelength (308 nm) in THF solution. It is only slightly soluble in alkanes but dissolves readily in THF and benzene.

Flash photolysis (308 nm) of a cyclohexane solution of **1Os** (ca. 8×10^{-5} mol dm^{-3}) under argon resulted in a transient absorption with an instrument-limited risetime (ca. 100 ns). The maximum absorption was observed at approximately 390 nm (Figure 3), with no further absorption maxima at longer

Table 3. Second-Order Rate Constants for Reaction of $M(PP_3)$ (M = Ru, Os) with Quenchers at 296 K

quencher[a]	gas solubility[b]/ mol dm^{-3} atm^{-1}	k/dm^3 mol^{-1} s^{-1} $Ru(PP_3)$[c]	k/dm^3 mol^{-1} s^{-1} $Os(PP_3)$[c]
H_2	3.8×10^{-3}	$(2.0 \pm 0.4) \times 10^6$	
cyclohexane			1.5×10^{3}[d]
cyclohexane-d_{12}			5.3×10^{2}[d]
pentane			$(6.0 \pm 1.0) \times 10^4$
heptane			$(9.5 \pm 1.4) \times 10^4$
methylcyclohexane			$(3.1 \pm 0.5) \times 10^4$
methylcyclohexane-d_{14}			$(5.5 \pm 1.5) \times 10^3$
benzene		$(1.3 \pm 0.1) \times 10^6$	$(3.2 \pm 0.5) \times 10^5$
benzene-d_6		$(6.8 \pm 0.7) \times 10^5$	$(5.7 \pm 1.0) \times 10^5$
THF		$(1.6 \pm 0.2) \times 10^6$	$(3.2 \pm 0.6) \times 10^5$
THF-d_8		$(1.5 \pm 0.1) \times 10^6$	$(4.5 \pm 1.1) \times 10^5$
$HSiEt_3$		$(5.4 \pm 1.1) \times 10^5$	$(3.3 \pm 0.7) \times 10^5$
CO	9.3×10^{-3}	$(1.0 \pm 0.1) \times 10^6$	6.5×10^5
ethene	0.14	7.6×10^5	$(3.2 \pm 0.4) \times 10^5$
N_2	7.1×10^{-3}	$(7.5 \pm 1.8) \times 10^5$	2.2×10^6
methane	3.0×10^{-2}		$(2.6 \pm 0.4) \times 10^5$

[a] All measurements were taken in cyclohexane solution. [b] Reference 21 for gas solubility. [c] Error bars as 95% probability on least squares fit. When no error bars are shown, rate constant based on measurements with 1 atm gas only. [d] The rate constants for reaction with cyclohexane are taken from measurements in neat cyclohexane.

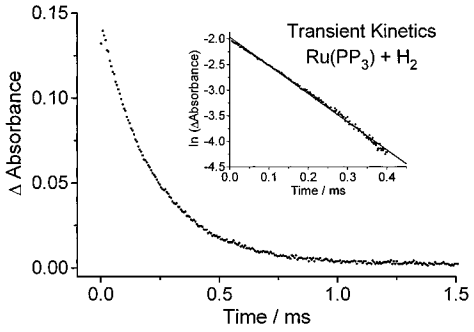

Figure 4. Decay of the transient formed on the flash photolysis of $Ru(PP_3)H_2$ in cyclohexane solution under 500 Torr of hydrogen + 260 Torr of argon. The decay is first-order (inset), and the signal decays to the baseline.

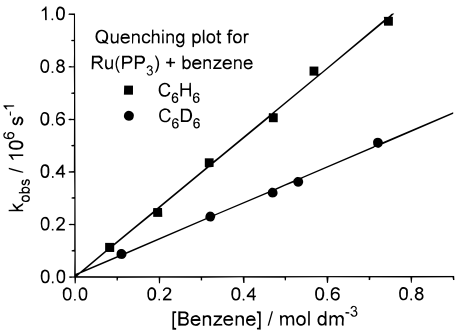

Figure 5. Plot of pseudo-first-order decay constant against concentration of benzene (■) and benzene-d_6 (●) for the transient formed on flash photolysis of $Ru(PP_3)H_2$.

wavelength. All subsequent kinetic data were recorded at 390 nm unless otherwise stated.

In cyclohexane under an argon atmosphere the transient signal decayed over several hundred microseconds and did not return to the baseline, indicating the formation of a longer-lived photoproduct. The decay was first-order as shown by the linearity of a plot of ln ΔA against time, $k_{obs} = 1.4 \times 10^4$ s^{-1}. The experiment was repeated in cyclohexane-d_{12}, and the pseudo-first-order rate constant, $k_{obs} = 4.9 \times 10^3$ s^{-1} was determined; thus the approximate kinetic isotope effect for this reaction is $k_H/k_D = 2.8$ (Table 4).[20]

When pentane was used as a solvent, a transient signal was observed with a similar λ_{max} to that observed in cyclohexane. However, the signal now decayed in just a few microseconds ($k_{obs} = 7.3 \times 10^5$ s^{-1}) and still did not return to the baseline. By varying the concentration of pentane in cyclohexane (0.24−1.32 mol dm^{-3}) and repeating the experiment it was found that k_{obs} varied linearly with pentane concentration (Figures 8 and 9a) giving a second-order rate constant of $(6.0 \pm 1.0) \times 10^4$ dm^3 mol^{-1} s^{-1} (Table 3). Similar experiments were undertaken with heptane (0.11−0.98 mol dm^{-3}), methylcyclohexane (0.08−1.26 mol dm^{-3}) (Table 3, Figure 9a), and methylcyclohexane-d_{14} (0.09−7.84 mol dm^{-3}) (Table 3). The results with methylcyclohexane allowed a kinetic isotope effect to be calculated of $k_H/k_D = 5.6 \pm 1.5$ (Table 4). The striking results with pentane, heptane, and methylcyclohexane led to investigation of methane as a quencher (see below).

In benzene solution, the decay of the transient formed on flash photolysis of **1Os** was too fast to observe. By varying the concentration of benzene in cyclohexane (0.12−0.94 mol dm^{-3}), it was shown that the rate of decay of the transient varied linearly with [benzene] (Table 3, Figure 9b). The experiments were repeated with benzene-d_6 (0.09−0.87 mol dm^{-3}) to give a second-order rate constant (Table 3, Figure 9b) and a kinetic isotope effect of $k_H/k_D = 0.6 \pm 0.1$ (Table 4). The quenching kinetics of **1Os** in cyclohexane with added $HSiEt_3$ (0.004−0.067 mol dm^{-3}) proved to be linear with respect to [$HSiEt_3$] (Table 3).

Quenching with tetrahydrofuran (0.006−0.060 mol dm^{-3}) yielded a double exponential decay (Figure 10a). The fast component showed a linear dependence on THF concentration (Table 3, Figure 10b). The longer-lived product (λ_{max} 440 nm) decayed with a first-order decay constant of $(4.2 \pm 0.8) \times 10^3$ s^{-1} which showed no dependence on the THF concentration (Figure 10c). Experiments with THF-d_8 (0.007−0.016 mol dm^{-3}) demonstrated similar double exponential behavior (Table 3). The longer-lived product decayed with a first-order decay constant of $(1.6 \pm 0.5) \times 10^3$ s^{-1} which again proved independent of [THF-d_8]. The resulting kinetic isotope effect for the fast component was not significant, but for the slow component the kinetic isotope effect is $k_H/k_D = 2.6 \pm 0.4$ (Table 4).

Quenching by hydrogen was investigated by preparing two samples of **1Os** in cyclohexane solution, under atmospheres of argon and hydrogen, respectively. The transient signals observed on flash photolysis decayed with identical rates. Even when the H_2 pressure was increased to 3 atm ([H_2] = 1.1×10^{-2} mol dm^{-3}), there was no change in the rate of decay relative to an argon atmosphere.

Quenching by CO was investigated by preparing two samples in cyclohexane under atmospheres of argon and CO respectively.

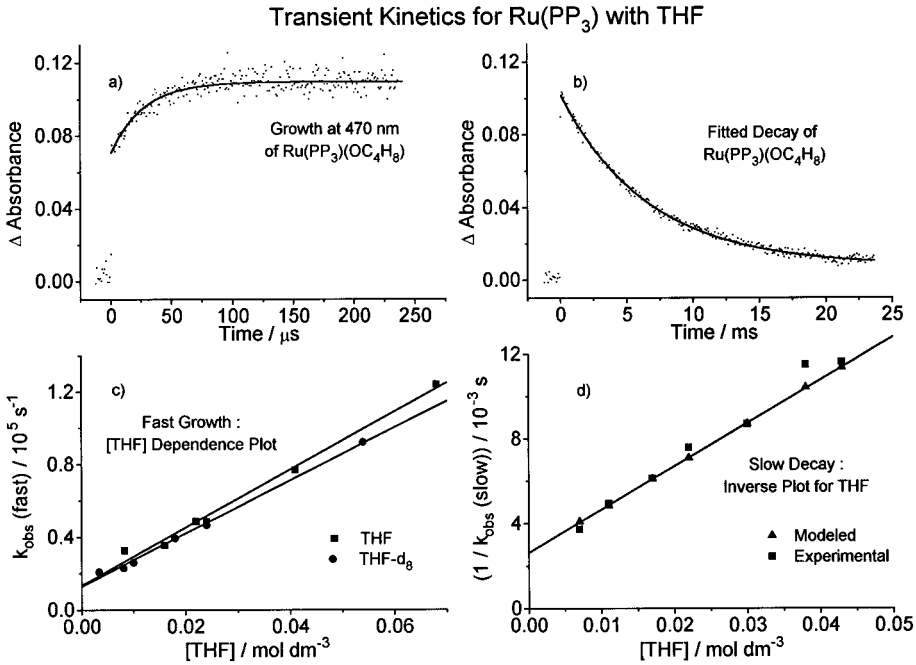

Figure 6. Analysis of photoreaction of Ru(PP$_3$)H$_2$ with THF in cyclohexane: (a) fitted data (λ = 470 nm, [THF-d_8] = 0.018 mol dm^{-3}) on short timescale, showing growth of Ru(PP$_3$)(OC$_4$H$_8$); (b) fitted data (λ = 470 nm, [THF-d_8] = 0.018 mol dm^{-3}) on long time scale, showing decay of Ru(PP$_3$)(OC$_4$H$_8$); (c) k_{obs} for fast growth against [THF] (■) and [THF-d_8] (●); and (d) 1/k_{obs} for slow decay against [THF] showing experimental data (■) and modeled data (▲).

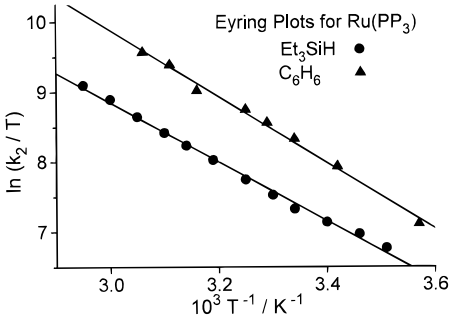

Figure 7. Eyring plots for the reaction of Ru(PP$_3$) with triethylsilane (●) and benzene (▲).

Scheme 9. Transient Photochemistry of Ru(PP$_3$)H$_2$

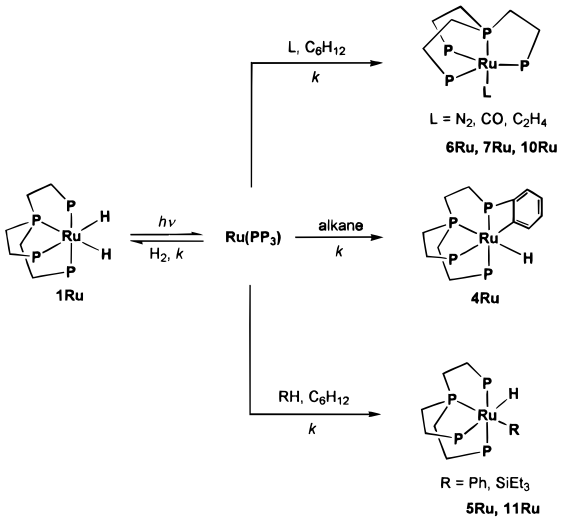

In the presence of CO, the decay was slightly, but reproducibly, faster (k_{obs} = 2.0 × 10^4 s^{-1}) than that under argon (k_{obs} = 1.4 × 10^4 s^{-1}). These data can be used to give an approximate value for the second-order rate constant for the reaction of the transient with CO (Table 3).

A similar experiment with a methane atmosphere showed that the transient decay was slightly faster under an atmosphere of methane than under argon ($k_{methane}$ = 2.2 × 10^4 s^{-1}, k_{argon} = 1.4 × 10^4 s^{-1}). The experiment was repeated with 2 and 3

Scheme 10. Transient Photochemistry of M(PP$_3$)H$_2$ in the Presence of THF: (a) M = Ru and (b) M = Os

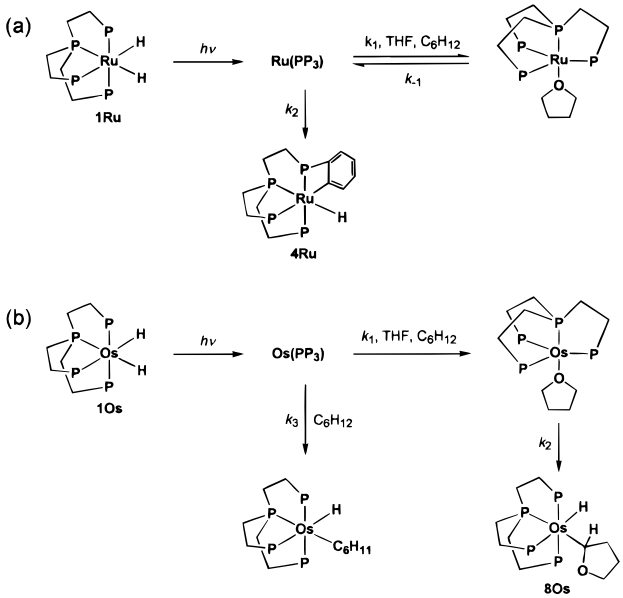

Table 4. Kinetic Isotope Effects (KIE) for the Reaction of M(PP$_3$) Transients with Selected Quenchers

quencher[a]	KIE Ru(PP$_3$)[b]	KIE Os(PP$_3$)[b]
cyclohexane		2.8
methylcyclohexane		5.6 ± 1.5
C_6H_6	1.5 ± 0.2	0.6 ± 0.1
THF: growth of M(PP$_3$)(OC$_4$H$_8$)	1.1 ± 0.2	0.7 ± 0.2
THF: decay of M(PP$_3$)(OC$_4$H$_8$)	0.9 ± 0.1	2.6 ± 0.4

[a] All measurements were taken in cyclohexane solution, except for cyclohexane where neat solvent was used. [b] Error bars as 95% probability on least squares fit. When no error bars are shown, rate constant based on measurements with one concentration only.

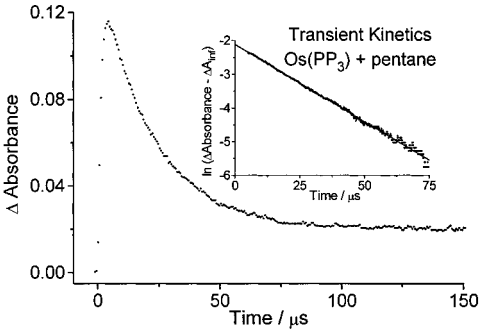

Figure 8. Decay of osmium transient in the presence of 0.47 mol dm^{-3} pentane in cyclohexane and first-order plot (inset). The decay is more than twice as fast as in cyclohexane alone.

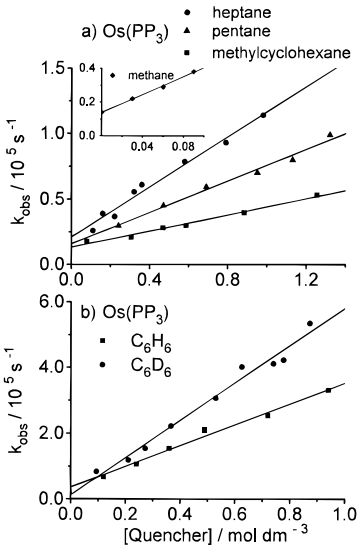

Figure 9. Plots of observed pseudo-first-order decay constant against quencher concentration for the decay of the transient formed on flash photolysis of $Os(PP_3)H_2$: (a) pentane (▲), heptane (●) and methylcyclohexane (■) inset: methane (◆); (b) benzene (■) and benzene-d_6 (●).

atm pressure of methane yielding a linear plot of k_{obs} against methane concentration (Table 3, Figure 9a, inset).

Quenching with nitrogen (1 and 2 atm) and ethene (60−760 Torr) was investigated (Table 3). The decays did not return to the baseline and had a large residual absorption.

The temperature dependences of the rate constants for the decay of the transient with pentane (1.64 mol dm^{-3}), triethylsilane (0.004−0.04 mol dm^{-3}), and benzene (0.19 mol dm^{-3}) were studied from 280−325, 283−337, and 287−326 K, respectively. Eyring plots of $\ln(k_2/T)$ against $1/T$ were used to extract the activation parameters (Tables 5 and S2, Figure S2).

The laser photochemistry of **1Os** can be interpreted in terms of $Os(PP_3)$ as the principal transient. The argument for the assignment is similar to that for $Ru(PP_3)$ except that the precursor is not regenerated under a hydrogen atmosphere. The quenching behavior is summarized in Scheme 11 for all quenchers except THF. Unlike $Ru(PP_3)$, the transient behavior of $Os(PP_3)$ provides direct evidence for reaction of heptane, pentane, methylcyclohexane, and methane. The kinetic isotope effect in cyclohexane provides evidence for the formation of $Os(PP_3)(C_6H_{11})H$, although the cyclometalated species (**4Os**) cannot be excluded as a possible product. The double exponential behavior in the presence of THF is suggestive of conversion of $Os(PP_3)$ to the oxygen-bound THF adduct, followed by conversion to the C−H insertion product (**80s**) observed by NMR. This sequence represented in Scheme 10b forms the basis for the fit to the kinetic data shown in Figure 10a. It also accounts for the kinetic isotope effect on the slower step but the lack of KIE on the fast step.

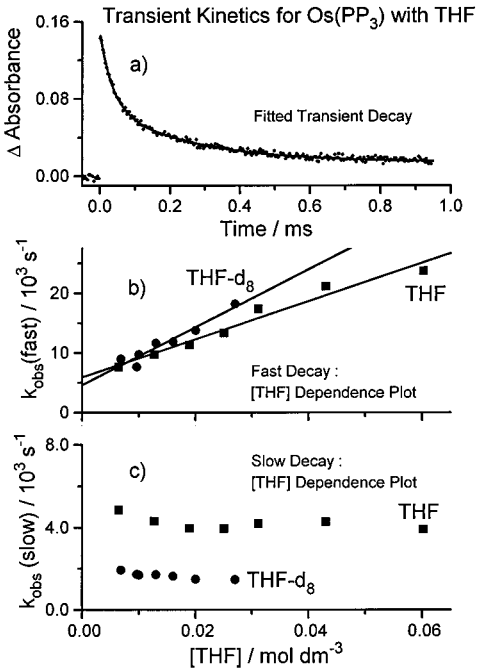

Figure 10. Analysis of photoreaction of $Os(PP_3)H_2$ with THF in cyclohexane: (a) fitted transient with [THF] = 0.025 mol dm^{-3}; (b) k_{obs} for fast decay against [THF] (■) and [THF-d_8] (●); (c) k_{obs} for slow decay against [THF] (■) and [THF-d_8] (●).

Table 5. Activation Parameters for the Reactions of $M(PP_3)$ (M = Ru, Os) and Related Compounds with Various Quenchers[a]

	$\Delta H^{\ddagger}$/ kJ mol^{-1}	$\Delta S^{\ddagger}$/ J mol^{-1} K^{-1}	$\Delta G^{\ddagger}_{298}$/ kJ mol^{-1}
$Ru(PP_3)$ + $HSiEt_3$	35 ± 2	−18 ± 6	40 ± 4
$Ru(PP_3)$ + benzene	39 ± 4	+1 ± 13	38 ± 6
$Os(PP_3)$ + pentane	27 ± 1	−59 ± 4	45 ± 2
$Os(PP_3)$ + $HSiEt_3$	31 ± 5	−27 ± 12	39 ± 6
$Os(PP_3)$ + benzene	38 ± 3	−7 ± 9	40 ± 4
$Ru(dmpe)_2$ + $HSiEt_3$[b]	9 ± 1	−53 ± 4	25 ± 2
$Fe(dmpe)_2$ + $HSiEt_3$[c]	22 ± 2	−87 ± 6	48 ± 3
$Ru(depe)_2$ + $HSiEt_3$[d]	11 ± 3	−112 ± 4	44 ± 1

[a] Error bars as 95% probability on least squares fit. [b] See ref 7. [c] See ref 24b. [d] See ref 8.

Scheme 11. Transient Photochemistry of $Os(PP_3)H_2$

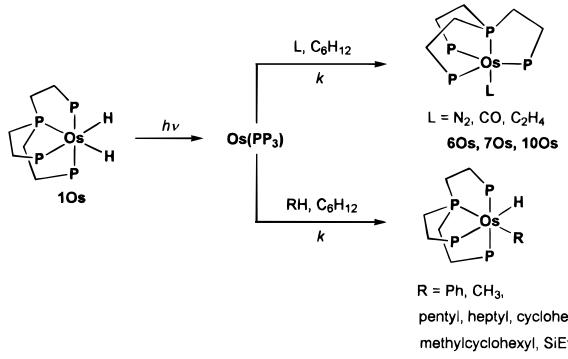

Discussion

The photochemistry of both $Ru(PP_3)H_2$ (**1Ru**) and $Os(PP_3)H_2$ (**1Os**) in solution proves to be extensive, leading to many products which can also be obtained by reductive synthesis from $M(PP_3)Cl_2$ (**2Ru**/**2Os**). In some cases the photochemical route is preferred, while reductive routes are more facile for others.

Product Studies. Photolysis of **1Ru** in THF under a rigorously inert atmosphere yields the cyclometalated complex

(**4Ru**). This reacts readily with H_2 to regenerate **1Ru** and also acts as an efficient scavenger for N_2 to give Ru(PP$_3$)(N$_2$) (**6Ru**). Hence **4Ru** can be considered as a store for some of the photon energy in the absence of other quenchers. We deduce an order of thermodynamic stability: **4Ru** < **6Ru** < **1Ru**. However, Ru(PP$_3$)(Ph)H (**5Ru**) cannot be produced thermally by addition of benzene to a solution of **4Ru**. Ru(PP$_3$)(Ph)H is best formed photochemically at low temperature in THF/C_6H_6 mixtures, which also generates some of the cyclometalated species. Although dinitrogen complexes of Ru(II) are abundant, **6Ru** is a rare example of a dinitrogen complex of Ru(0).

The photochemistry of **1Os** proved substantially different from its ruthenium analogue. Photolysis in THF yielded the tetrahydrofuranyl hydride complex (**8Os**), which could also be formed by reductive synthesis from Os(PP$_3$)Cl$_2$, and has no ruthenium analogue. Secondary photolysis of **8Os** was found to be the only route to the cyclometalated complex (**4Os**). The formation of Os(PP$_3$)(N$_2$) (**6Os**) proved inaccessible by photochemical routes. However, **6Os** could be generated in THF at low temperature by a thermal method but reacted with THF upon warming. Finally, in contrast to the ruthenium analogue, Os(PP$_3$)(Ph)H (**5Os**) is thermally stable and can be obtained by both photochemical and reductive routes.

Dahlenburg et al. have studied the reduction of a variety of related MP$_4$Cl$_2$ (M = Ru, Os) complexes in which the phosphines have methyl rather than phenyl substituents.[22] They have employed the tetradentate phosphines P(CH$_2$CH$_2$CH$_2$PMe$_2$)$_3$ (P$_4^A$), P((C$_6$H$_4$)PMe$_2$)$_3$ (P$_4^B$), and combinations of bi- and tridentate phosphines with PMe$_3$. The RuP$_4$Cl$_2$ species invariably yield RuP$_4$(Ph)H on reduction in the presence of benzene, while a photochemical route from the dihydride has also been employed for Ru(P$_4^A$)(Ph)H. Unlike our Ru(PP$_3$)(Ph)H these are stable, isolable complexes. The reduction of Ru(P$_4^A$)Cl$_2$ in THF yields Ru(P$_4^A$)(2-C$_4$H$_7$O)H, which is an exact analogue of **8Os**.

The methyl hydride complex, Os(PP$_3$)(Me)H, was generated from Os(PP$_3$)(OTf)H in benzene solution but proved unstable with respect to Os(PP$_3$)(Ph)H. The low solubility of Os(PP$_3$)H$_2$ prevented us from carrying out product studies by NMR in alkane solvents.

For comparison, Flood et al. have studied the thermolysis of Os(PMe$_3$)$_4$(CH$_2$CMe$_3$)H with hydrocarbons, isolating C−H activation products, Os(PMe$_3$)$_4$(R)H, from benzene, Me$_4$Si, mesitylene, and methane.[23] In the absence of these substrates a cyclometalation product is formed. The reaction with benzene proceeds via oxidative addition of benzene to Os(PMe$_3$)$_3$(CH$_2$CMe$_3$)H to form an Os^{IV} intermediate, whereas reaction with Me$_4$Si involves oxidative addition to Os(PMe$_3$)$_3$.

Transient Photochemistry. Laser flash photolysis of M(PP$_3$)H$_2$ yields transients within the instrumental risetime (ca. 100 ns) which are assigned to M(PP$_3$). They exhibit a single absorption maximum at 395 nm (M = Ru) and 390 nm (M = Os), respectively. These spectra contrast with those of Ru(drpe)$_2$[8] and Os(dmpe)$_2$,[24a] all of which show a series of absorption bands across the visible spectrum including one at very long wavelength between 700 and 800 nm. We deduce that the C_{3v} or C_s geometry (Scheme 1) enforced by the tetradentate PP$_3$ ligand removes the long wavelength bands characteristic of the square planar geometry adopted by the M^0 complexes with two bidentate phosphine ligands. An additional influence on the UV/visible spectrum may come from an interaction of the metal with a phenyl group of the PP$_3$ ligand (see below). These conclusions are also consistent with observations on Fe(dmpe)$_2$ which exhibits a UV/visible spectrum with a single maximum at 390 nm.[24b] The proposed geometry of the transient Fe(dmpe)$_2$ is C_s rather than the square planar D_{2h} for the ruthenium analogues.

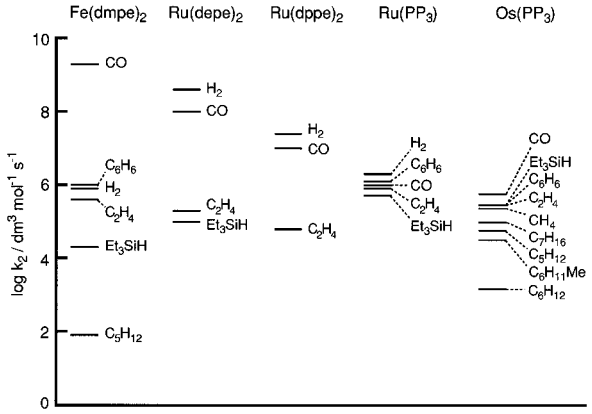

Figure 11. Schematic diagram showing the rate constants for reaction of M(PP$_3$) compared to those for Fe(dmpe)$_2$, Ru(dppe)$_2$, and Ru(depe)$_2$.

Reactivity of Transients. The rate constants for reaction of M(PP$_3$) are shown schematically in Figure 11, together with those for Fe(dmpe)$_2$, Ru(depe)$_2$, and Ru(dppe)$_2$. A notable feature is the narrow range of rate constants, varying for Ru(PP$_3$) between 5.4×10^5 and 2.0×10^6 dm^3 mol^{-1} s^{-1} and for Os(PP$_3$) between 1.5×10^3 and 6.5×10^5 dm^3 mol^{-1} s^{-1}. This lack of selectivity contrasts with the behavior of Ru(dppe)$_2$ and Ru(depe)$_2$.[8] Thus the ratio of rate constants for reaction with H_2 and C_2H_4, $k(H_2)/k(C_2H_4)$ is 2.6 for Ru(PP$_3$) but 410 for Ru(dppe)$_2$. The comparison with selectivity for H_2 over HSiEt$_3$ is even more dramatic: $k(H_2)/k(HSiEt_3)$ is 3.7 for Ru(PP$_3$) but 3600 for Ru(depe)$_2$.

The reactivity of Ru(PP$_3$) is also enhanced toward some key substrates compared to Ru(depe)$_2$ and Ru(dppe)$_2$. The species with the tetradentate ligand reacts rapidly with HSiEt$_3$ and benzene. The closest analogue with bidentate ligands, Ru(dppe)$_2$, reacts with neither HSiEt$_3$ nor C_6H_6 in the presence of photogenerated hydrogen. Ru(depe)$_2$ reacts with HSiEt$_3$ but not with C_6H_6. Thus the striking reactions of Ru(PP$_3$) are as a result of reduced selectivity for hydrogen coupled with enhanced reactivity toward other species.

When we consider Os(PP$_3$), the changed reactivity is even more remarkable. The back reaction of Os(PP$_3$) with H_2 fails to compete with solvent activation even under 3 atm H_2. Instead we observe a first-order decay of the transient in cyclohexane with a rate constant of 1.4×10^4 s^{-1}. This measurement enables us to calculate an upper limiting rate constant for reaction of Os(PP$_3$) with H_2 of ca. 10^6 dm^3 mol^{-1} s^{-1}. The rate constants for reaction of Os(PP$_3$) with CO, HSiEt$_3$, and ethene are all reduced marginally relative to Ru(PP$_3$). However, the striking feature is that Os(PP$_3$) reacts with alkanes containing a primary alkyl group and with methane itself. The rate constants increase in the order methylcyclohexane < pentane < heptane < methane < benzene. The large kinetic isotope effect for the reaction with methylcyclohexane (k_H/k_D = 5.6) provides evidence that the observed quenching by alkanes involves C−H bond breaking and the formation of new alkyl hydride species. Remarkably, the rate constant for reaction with methane is only about 20%

(22) (a) Antberg, M.; Dahlenburg, L. *J. Organomet. Chem.* **1986**, *312*, C67. (b) Dahlenburg, L.; Frosin, K.-M. *Chem. Ber.* **1988**, *121*, 865. (c) Dahlenburg, L.; Kerstan, S.; Werner, D. *J. Organomet. Chem.* **1991**, *411*, 457.

(23) (a) Desrosiers, P. J.; Shinomoto, R. S.; Flood, T. C. *J. Am. Chem. Soc.* **1986**, *108*, 1346 and 7964. (b) Harper, T. G. P.; Shinomoto, R. S.; Deming, M. A.; Flood, T. C. *J. Am. Chem. Soc.* **1988**, *110*, 7915. (c) Shinomoto, R. S.; Desrosiers, P. J.; Harper, T. G. P.; Flood, T. C. *J. Am. Chem. Soc.* **1990**, *112*, 704. (d) Ermer, S. P.; Shinomoto, R. S.; Deming, M. A.; Flood, T. C. *Organometallics* **1989**, *8*, 1377.

(24) (a) Nicasio, M. C.; Perutz, R. N. Unpublished observations. (b) Whittlesey, M. K.; Mawby, R. J.; Osman, R.; Perutz, R. N.; Field, L. D.; Wilkinson, M. P.; George, M. W. *J. Am. Chem. Soc.* **1993**, *115*, 8627.

lower than that with benzene. The kinetic isotope effect measured for the reaction of $Os(PP_3)$ with cyclohexane ($k_H/k_D = 2.8$) suggests that the transient is even capable of activating secondary C−H bonds in the absence of more reactive substrates, despite the possibility for intramolecular activation to form the cyclometalated species. The rate constant for reaction with cyclohexane is, however, at least 20 times smaller than that for the reaction with alkanes containing methyl groups. It is this selectivity which has enabled us to determine full kinetic quenching plots for reactions with alkanes in the presence of cyclohexane as solvent. Thus $Os(PP_3)$ brings reduced reactivity toward H_2 but enhanced reactivity toward alkanes, with substantial selectivity for CH_4 over primary C−H bonds, and primary over secondary C−H bonds.

Kinetic selectivities for different alkanes have been determined previously for Tp′Rh(CNR) (Tp′ = HB(3,5-dimethylpyrazolyl)$_3$). The selectivity for primary over secondary C−H bonds of $Os(PP_3)$ is at least five times higher than that for Tp′Rh(CNR) which previously displayed the highest kinetic selectivities for hydrocarbons.[25] The kinetic selectivities are calculated as a ratio of the rate constants for the hydrocarbon involved and normalized with respect to the number of C−H bonds of interest present in the hydrocarbon. The kinetic selectivity of $Os(PP_3)$ for methane over cyclohexane is at least 520 times greater than for Tp′Rh(CNR), where reaction with methane was not observed at atmospheric pressure. Reactions of osmium complexes with alkanes, including methane, have been recorded previously in arene half-sandwich complexes[6] and in other phosphine complexes.[23]

The reactions of $M(PP_3)$ with THF require analysis of more complex kinetics. For $Ru(PP_3)$ the oscilloscope traces measured at 470 nm (near the maximum for the O-bound THF adduct) showed a rapid growth (ca. 10^{-5} s, Figure 6a) followed by a slow decay (ca. 10^{-2} s, Figure 6b). Each trace could be fitted to a simple exponential function to yield k_{obs}(fast) for the growth, or k_{obs}(slow) for the decay. The data were analyzed according to the mechanism of Scheme 10a. A plot of k_{obs}(fast) versus [THF] was linear and yielded the rate constant for reaction of $Ru(PP_3)$ with THF to form an O-bound adduct, $k_1 = (1.6 \pm 0.2) \times 10^6$ dm^3 mol^{-1} s^{-1} (Figure 6c). A plot of $1/k_{obs}$(slow) versus THF was linear. This reciprocal plot could be modeled most satisfactorily when $k_{-1} = 2 \times 10^4$ s^{-1} and $k_2 = 400$ s^{-1} (Figure 6d). The kinetic modeling does not represent a unique solution but is consistent with the measurements in pure cyclohexane which give a value for k_{obs} of 350 s^{-1}. This slow step is attributed to cyclometalation of the fragment. The values of k_1 and k_{-1} combine to give an equilibrium constant for formation of $Ru(PP_3)$(THF) of ca. 80. The lifetime of $Ru(PP_3)$(THF) in pure THF of ca. 200 ms also suggests a weakly bound adduct.

The reactivity of $Os(PP_3)$ in THF follows a different pattern. The kinetics are fitted to Scheme 10b. The model was fitted using an analytical expression[26] for multistep irreversible reactions, as derived from the first-order differential equations. Here, trapping of $Os(PP_3)$ to form an oxygen bound adduct (which displays no kinetic isotope effect, Tables 3 and 4) competes with the decay process found in pure cyclohexane (which is probably C−H activation, see earlier). The oxygen bound adduct converts to $Os(PP_3)$(tetrahydrofuranyl)H with a rate constant of $k_2 = 4.2 \times 10^3$ s^{-1}. This step exhibits a kinetic isotope effect of $k_H/k_D = 2.6 \pm 0.4$. We also considered a reaction scheme in which the oxygen-bound adduct is formed reversibly and $Os(PP_3)$(tetrahydrofuranyl)H is formed directly from $Os(PP_3)$. However, we were unable to obtain a rate dependence on the THF concentration which was consistent with the observed KIE for the second mechanism.

The kinetic isotope effects are collected in Table 4. All significant KIEs are normal except for $Os(PP_3)$ with benzene for which an inverse effect is observed ($k_H/k_D = 0.6 \pm 0.1$). Inverse isotope effects are usually interpreted in terms of a preequilibrium to form an η^2-C_6H_6 complex. However, ab initio calculations of kinetic isotope effects suggest a considerable need for caution in deducing mechanisms from inverse kinetic isotope effects.[27]

The differing reactivities of $M(PP_3)$ and $Ru(drpe)_2$ should be apparent through activation parameters. The enthalpies of activation (Table 5) vary between 35 and 39 kJ mol^{-1} for $Ru(PP_3)$ and between 27 and 38 kJ mol^{-1} for $Os(PP_3)$. All these values are much higher than those for reactions of $Ru(dmpe)_2$ or $Ru(depe)_2$ with $HSiEt_3$. The entropies of activation are surprisingly close to zero for bimolecular processes, the most negative being for $Os(PP_3)$ + pentane. The small value of $\Delta S^{\ddagger}$ for $Ru(PP_3)$ and $HSiEt_3$ contrasts with much more negative values for the reactions of the bidentate analogues. The entropies of activation for $M(PP_3)$ + $HSiEt_3$ are similar to that for $CpMn(CO)_2S$ (S = solvent) + $HSiEt_3$ (-28 ± 10 J K^{-1} mol^{-1}),[28] which has been interpreted in terms of an early transition state.

Key differences in the reactivity of $Ru(PP_3)$ and $Os(PP_3)$ may be summarized as follows: (a) $Ru(PP_3)$ cyclometalates thermally, $Os(PP_3)$ cyclometalates only via secondary photolysis of **8Os**; (b) $Ru(PP_3)$ reacts with H_2 under our conditions, $Os(PP_3)$ does not; and (c) only $Os(PP_3)$ undergoes C−H activation reactions with alkanes and THF. The ability to undergo C−H activation reactions is associated with the increased strength of M−H and M−C bonds among the third row elements.[29]

Structural Implications of Reactivity. The reactivity patterns of $M(PP_3)$ may be summarized as low selectivity with reduced reactivity toward H_2 but enhanced reactivity toward other substrates relative to $Ru(drpe)_2$. Where comparisons are possible, the value of $\Delta H^{\ddagger}$ is higher than for $Ru(drpe)_2$ and the value of $\Delta S^{\ddagger}$ is less negative. We have considered three explanations of these phenomena involving (i) a spin triplet ground state, (ii) specific solvation, and (iii) a barrier created by the position of the phosphine phenyl groups.

The possibility of a triplet ground state for $M(PP_3)$ requires serious consideration since $Co(NP_3)^+$ ($NP_3 = N(CH_2CH_2PPh_2)_3$) exhibits such a ground state in the solid phase.[30a] However, spin crossover effects should result in an entropic barrier as for $Fe(CO)_4$.[30b] Moreover, the absence of a heavy atom effect when

(25) Jones, W. D.; Hessel, E. T. *J. Am. Chem. Soc.* **1993**, *115*, 554.

(26) The analytical equation derived for fitting the double exponential decay traces (Figure 10a) to the proposed mechanism (Scheme 10b) for the reaction of $Os(PP_3)$ in the presence of THF is shown below:

$$\Delta A = e^{-(k_1+k_3)t}\left\{a + \frac{bk_1}{(k_2-k_1-k_3)} - \frac{ck_1k_3}{(k_2-k_1-k_3)(k_1+k_3)} - \frac{dk_3}{(k_1+k_3)}\right\} + e^{-k_2t}\left\{\frac{(c-b)k_1}{(k_2-k_1-k_3)}\right\} + \frac{ck_1+dk_3}{(k_1+k_3)}$$

where k_1 is the pseudo-first-order rate constant and k_3 was assumed to take the same value as that observed in neat cyclohexane (1.4×10^4 s^{-1}). The other variables are defined as $a = \epsilon(Os(PP_3)) \times [Os(PP_3)]_0$; $b = \epsilon(Os(PP_3)(OC_4H_8)) \times [Os(PP_3)]_0$; $c = \epsilon(Os(PP_3)(2\text{-}C_4H_7O)H) \times [Os(PP_3)]_0$; and $d = \epsilon(Os(PP_3)(C_6H_{11})H) \times [Os(PP_3)]_0$ where $[Os(PP_3)]_0$ is the initial concentration of $Os(PP_3)$ generated by the laser. The values of k_1, k_2, a, b, c, and d were fitted to the observed kinetic traces for each concentration of THF.

(27) (a) Abu-Hasanayn, F.; Goldman, A. S.; Krogh-Jesperson, K. *J. Phys. Chem.* **1993**, *97*, 5890. (b) Hall, C.; Perutz, R. N. *Chem. Rev.* **1996**, *96*, 3125.

(28) Hill, R. H.; Wrighton, M. S. *Organometallics* **1987**, *6*, 632.

(29) Martinho-Simoes, J. A.; Beauchamp, J. C. *Chem. Rev.* **1990**, *90*, 629.

(30) (a) Sacconi, L.; Orlandini, A.; Midollini, S. *Inorg. Chem.* **1974**, *13*, 2850. (b) Weitz, E. *J. Phys. Chem.* **1987**, *91*, 3945.

Xe was dissolved in a solution of Ru(PP$_3$)H$_2$ + CO lends no support to this hypothesis. Of course, high spin ground states for ruthenium and osmium complexes would be highly unusual. For these reasons a spin triplet ground state for M(PP$_3$) is excluded.

The presence of a solvent molecule coordinated to a reactive intermediate is characteristic of many d^6 species such as Cr(CO)$_5$S (S = solvent)[31] and CpMn(CO)$_2$S.[32] Solvent coordination has also been observed for Ru(CO)$_2$(PMe$_3$)$_2$S[33] but not for Ru(drpe)$_2$. If this model is correct, the barrier to reaction would arise principally by displacement of the solvent molecule by the incoming substrate. Since M(PP$_3$) species are so reactive and the parent dihydrides are not soluble in perfluoroalkanes, this model has proved hard to test. We note that the rate constant for reaction of Ru(PP$_3$) with H$_2$ increased significantly between cyclohexane and heptane as solvents, but the change was within the limits of general solvent effects.

In the third model, motion of the phenyl groups to a less favorable conformation where they are out of the way of an incoming ligand gives rise to the high $\Delta H^{\ddagger}$, and an early transition state, and hence low $\Delta S^{\ddagger}$. The steric effects of the phenyl groups in either C_{3v} or C_s structures may be modeled by an examination of the crystal structures of analogous 18 electron rhodium and iridium complexes.[34] Moreover, there is the additional possibility that a phenyl group may act as an agostic ligand to ruthenium or osmium in M(PP$_3$). The plausibility of an agostic interaction is made clear by model building and by analogy with the structures of [Re(triphos)(CO)$_2$]BF$_4$ (triphos = MeC(CH$_2$PPh$_2$)$_3$)[35] and Ru(PPh$_3$)$_3$Cl$_2$.[36] If correct, the agostic interaction will certainly affect the UV/visible spectrum of M(PP$_3$). Although the agostic model cannot be distinguished experimentally at this stage from solvent coordination, we consider that it offers the most satisfactory explanation of the observed behavior.

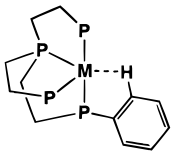

Conclusion

A range of complexes, M(PP$_3$)L and M(PP$_3$)(X)Y (M = Ru, Os), have been synthesized by reduction of M(PP$_3$)Cl$_2$ and by photolysis of M(PP$_3$)H$_2$. The transient intermediates, M(PP$_3$), have been detected by laser flash photolysis, and the kinetics of their reactions with a range of substrates have been determined. Key features are summarized below: (a) Photolysis of Ru(PP$_3$)H$_2$ in THF under an inert atmosphere yields the cyclometalated complex (**4Ru**), which acts as an energy store, and scavenges N$_2$ and H$_2$. (b) Photolysis of Os(PP$_3$)H$_2$ in THF yields the tetrahydrofuranyl hydride complex (**8Os**), which is better synthesized reductively. The cyclometalated osmium complex (**4Os**) is only formed on photolysis of **8Os**. (c) Benzene activation leads to formation of M(PP$_3$)(Ph)H complexes. The osmium product is isolable, but the ruthenium product is thermally labile. Os(PP$_3$)(Me)H has been synthesized but proves unstable with respect to reductive elimination of methane. (d) The UV/visible spectra of the M(PP$_3$) intermediates are quite different from the square planar transients such as Ru(dppe)$_2$. The change reflects the enforced C_{3v} or C_s structure and the likely agostic interaction of a phenyl group. (e) The reactivity of Ru(PP$_3$) is quite different from Ru(dppe)$_2$ and Ru(depe)$_2$ with a more rapid reaction with HSiEt$_3$ but a much slower reaction with H$_2$. Of these three transients, only Ru(PP$_3$) reacts with benzene. (f) Os(PP$_3$) inserts into C−H bonds of alkanes in addition to those of benzene and THF. The high sensitivity of UV/visible spectroscopy coupled with the use of kinetic isotope effects enable these reactions to be established despite very low solubility of the precursors in alkanes. The rate constants follow the order: cyclohexane < methylcyclohexane < pentane < heptane < methane < benzene ≈ THF. The selectivity for primary alkyl groups and methane over cyclohexane is sufficient that full quenching experiments can be carried out. The rate of reaction with methane is only about 20% slower than that with benzene. (g) The enforced C_{3v} or C_s structure successfully prepares Ru(PP$_3$), and more especially Os(PP$_3$), for C−H activation. The barrier to intermolecular C−H or Si−H activation must be lower than for square planar analogues because of the prearranged geometry. Most remarkably, the barrier to cyclometalation is high enough that this process does not compete effectively with intermolecular processes for Ru(PP$_3$) and is only accessible photochemically for Os(PP$_3$). It is equally significant that the reactions of M(PP$_3$) with H$_2$ are not fast enough to inhibit C−H activation.

Acknowledgment. The York group thanks EPSRC and British Gas for financial support, while the Florence group thanks the EC for support (contract ERB CHRXCT 930147). We appreciated helpful discussions with Dr M. K. Whittlesey and Dr M. C. Nicasio and would like to acknowledge Prof. K. G. Caulton for bringing an error in our communication to our attention. Thanks are expressed to Mr F. Zanobini for his assistance in the synthesis of the starting materials and Miss C. L. Higgitt for running NMR spectra in York.

Supporting Information Available: Tables S1 and S2 show the temperature dependence data for flash photolysis with Ru(PP$_3$) and Os(PP$_3$), respectively and Figures S1 and S2 show quenching of Ru(PP$_3$) with gaseous quenchers and Eyring plots for Os(PP$_3$), respectively (5 pages). See any current masthead page for ordering and Internet access instructions.

JA963797W

(31) (a) Kelly, J. M.; Long, C.; Bonneau, R. *J. Phys. Chem.* **1983**, *87*, 3344. (b) Wang, L.; Zhu, X.; Spears, K. G. *J. Am. Chem. Soc.* **1988**, *110*, 8695.

(32) Creaven, B. S.; Dixon, A. J.; Kelly, J. M.; Long, C.; Poliakoff, M. *Organometallics* **1987**, *6*, 2600.

(33) Mawby, R. J.; Perutz, R. N.; Whittlesey, M. K. *Organometallics* **1995**, *14*, 3268.

(34) (a) Di Varia, M.; Rovai, D.; Stoppioni, P.; Peruzzini, M. *J. Organomet. Chem.* **1991**, *420*, 135. (b) Bianchini, C.; Masi, D.; Mealli, C.; Meli, A.; Sabat, M. *Organometallics* **1985**, *4*, 1014. (c) Di Varia, M.; Peruzzini, M.; Stoppioni, P. *Inorg. Chem.* **1991**, *30*, 1001.

(35) Bianchini, C.; Marchi, A.; Marvelli, L.; Peruzzini, M.; Romerosa, A.; Rossi, R.; Vacca, A. *Organometallics* **1995**, *14*, 3203.

(36) La Placa, S. J.; Ibers, J. A. *Inorg. Chem.* **1965**, *4*, 778.